Tampere University

Timo Punkari

MONOLITHIC SUPERCAPACITOR FABRICATION WITH SCREEN-PRINTING

Master's Thesis
Faculty of Information Technology and Communication Sciences
Examiners: Prof. Matti Mäntysalo
Dr. Jari Keskinen
September 2023

ABSTRACT

Timo Punkari: Monolithic supercapacitor fabrication with screen-printing
Master's Thesis
Tampere University
Electrical Engineering
September 2023

Supercapacitors are generally used as electrical energy storage. An electrochemical double layer in the supercapacitor causes high capacitance. Compared to batteries supercapacitors have lower energy density but higher power density, longer lifetime, and wider operating temperature. Additionally, materials for supercapacitors can be chosen to be more environmentally sustainable and non-toxic. Recently research has widely investigated different materials to improve the energy density of supercapacitors. Because of the lower energy density, supercapacitors cannot supersede batteries alone. Together with energy harvesting, supercapacitors can establish energy autonomous systems. Furthermore, hybrid systems can be made from batteries and supercapacitors to exploit the benefits of both devices. [1,2]

The thesis aimed to use screen-printing to fabricate a supercapacitor with a monolithic structure. The structure has all layers; 1st current collector, 1st electrode, separator, 2nd electrode, and 2nd current collector printed on top of each other. This way the fabrication process does not require an assembly step, in which the separator, electrolyte and two electrodes are merged. However, the separator must prevent contact between the electrodes in the monolithic structure already during the fabrication. Inks for the supercapacitor layers were tested with the screen-printer. The separator layer turned out to be challenging, thus different printing practices were studied.

In the thesis, the monolithic supercapacitor was successfully fabricated with a screen-printer. The achieved separator in the monolithic structure corresponded with the commercial paper used as the separator. Printed separators prevented short circuits and demonstrated low leakage current of 4.6 µA in the supercapacitors. However, the discovered fabrication process for the separator layer requires in total six prints and the layer was cured twice between the prints. In future work, the printing process should be further developed in a way that the process would be simpler and would achieve smoother layers. Especially, the separator layer has a rough surface which influenced the upper electrode layer. Fabricated supercapacitors had variations in the capacitance, which are believed to occur from uneven electrodes.

Keywords: Supercapacitor, Ultracapacitor, Electric double-layer capacitor, Separator, Printed electronics, Screen-printing, Monolithic integration

TIIVISTELMÄ

Timo Punkari: Monoliittisen superkondensaattorin valmistus silkkipainomenetelmällä
Diplomityö
Tampereen yliopisto
Sähkötekniikka
Syyskuu 2023

Superkondensaattori on tyypillisesti sähköenergian varastointiin käytetty komponentti, jonka suuri kapasitanssi saavutetaan sähkökemiallisen kaksoiskerroksen avulla. Verrattuna yleisempään akkuun superkondensaattorin energiatiheys on pieni, mutta esimerkiksi tehotiheys, käyttöikä ja toimintalämpötila ovat suurempia. Erilaisia materiaaleja on tutkittu paljon superkondensaattoreissa suuremman energiatiheyden saavuttamiseksi. Lisäksi superkondensaattoreiden materiaalit voidaan valita ympäristön kannalta kestävästi ja välttää haitallisia materiaaleja. Koska energiatiheys on heikompi kuin akuilla, eivät superkondensaattorit voi täysin korvata akkuja. Toisaalta energiakeräimen kanssa superkondensaattori voi muodostaa energiaomavaraisen laitteen. Lisäksi superkondensaattori sekä akku on mahdollista yhdistää sovelluksessa, jolloin molempien sähköenergiavarastojen ominaisuuksia voidaan hyödyntää. [1,2]

Työn tavoitteena oli valmistaa superkondensaattori silkkipainomenetelmällä siten, että rakenteessa kerrokset on painettu toistensa päälle muodostaen monoliittisen rakenteen. Tällä tavalla voidaan välttää kokoamisvaihe, jossa erilliset elektrodipuolikkaat ja separaattori yhdistetään. Rakenteessa, jossa kaikki superkondensaattorin kerrokset (1. virrankerääjä, 1. elektrodi, separaattori, 2. elektrodi, 2. virrankerääjä) painetaan, on separaattorin estettävä yhteys elektrodien välillä jo valmistusvaiheessa. Eri kerrosten musteet testattiin painaa alkuun silkkipainokoneella. Separaattori kerroksen muodostaminen osoittautui haastavaksi ja täten erilaisia painokäytänteitä tutkittiin.

Työssä onnistuttiin valmistamaan monoliittinen superkondensaattori silkkipainomenetelmällä. Saavutettu separaattori vastasi hyvin paperista separaattoria, kerros esti tehokkaasti oikosulut ja vuotovirta superkondensaattoreissa pysyi matalana 4,6 µA. Kuitenkin superkondensaattorin painoprosessi on pitkä, sillä separaattorikerros muodostuu kuudesta painatuksesta ja näiden välillä kerros on kuivattava kahdesti. Monoliittisen superkondensaattorin painoprosessia olisikin hyvä optimoida, jotta se olisi yksinkertaisempi sekä siten että kerrokset olisivat tasaisempia. Eritoten separaattorikerroksen havaittiin jäävän karheaksi, mikä hankaloitti saamaan tasaisia elektrodikerroksia. Valmistetuissa superkondensaattoreissa havaittiinkin eroavaisuuksia kapasitansseissa ja näiden arvellaan johtuvan nimenomaan elektrodikerroksen vaihtelevuudesta.

Avainsanat: Superkondensaattori, Ultrakondensaattori, Separaattori, Painettava elektroniikka, Silkkipaino, Monoliittinen integraatio

PREFACE

This Master's Thesis was written at Faculty of Information Technology and Communication Sciences at Tampere University. I would like to thank for help and guidance my thesis instructors and examiners, Prof. Matti Mäntysalo and Dr. Jari Keskinen. The thesis is written from research done in the InComEss project, which has received funding from the European Union's Horizon 2020 research and innovation programme under grand agreement number 862597. Parts of the research used Academy of Finland Research Infrastructure "Printed Intelligence Infrastructure".

I am also grateful to all members of the Laboratory for Future Electronics from Tampere University for all help. Lastly, I appreciate all the support from family members and friends.

Tampere, 9 September 2023

Timo Punkari

CONTENTS

LIST OF SYMBOLS AND ABBREVIATIONS

AC	*Activated carbon*
C&E	*Cause and Effect*
CCCD	*Constant current charge discharge*
CV	*Cyclic voltammetry*
DC	*Direct current*
DI	*Deionized*
EDLC	*Electrochemical double layer capacitor*
EIS	*Electrochemical impedance spectroscopy*
ESR	*Equivalent series resistance*
F2F	*Face-to-face*
IPA	*Isopropyl alcohol*
PET	*Polyethylene terephthalate*
PI	*Polyimide*
R2R	*Roll-to-roll*
RMS	*Root mean square*
rpm	*Revolutions per minute*
SIPOC	*Suppliers, Inputs, Process, Outputs, and Customers*
UV	*Ultraviolet*
wt%	*Weight percentages*
σ	*standard deviation*
C	*capacitance*
C_s	*specific capacitance*
E	*energy*
I	*current*
m	*mean*
N	*sample size*
N_2	*nitrogen*
O_2	*oxygen*
q	*charge acceptance*
Q	*electrical charge*
R_a	*arithmetic average*
t	*time*
V	*voltage*
z	*height*

1. INTRODUCTION

Supercapacitors are electrical energy storage devices, owning high capacitance. Better known electrical energy storage devices are batteries, which have great energy density. However, general interest towards the supercapacitors is growing as those can provide alternative energy storage with higher power density and longer lifetime. Furthermore, most batteries contain harmful materials, but supercapacitors generally are more environmentally friendly. [1,3] Applications that require rapid charge or discharge are suitable for supercapacitors. Supercapacitors can stabilize transients and other instabilities in a grid. Electric vehicles also benefit from the supercapacitor advantages, but those cannot replace the battery fully as the low energy density does not fit for long-distance driving. On the other hand, use of the supercapacitors with energy harvesting has shown to be a promising concept and can supersede batteries in wireless sensor network applications. [1,4]

Research is mainly focused on the materials of the supercapacitors and especially on the electrode and electrolyte materials. Electrode materials are developed to achieve higher capacitance and different electrolytes to wider voltage windows. Research on the separator has been limited compared to these two. [1,2,5] Micro-supercapacitors with interdigitated electrodes highlight the absence of the separator, as the structure does not necessarily need the separator. Different fabrication techniques are already investigated for the micro-supercapacitors and reported with areal specific capacitance in the review article. [6] In a sandwich structure where two electrodes are assembled, the supercapacitor with activated carbon (AC) electrodes has been reported with a capacitance of 66 F g^{-1}. Previously, similar monolithic supercapacitors with AC electrodes have been reported to achieve over 200 mF capacitance on a cell. [7]

1.1 Aim and scope of the thesis

Motivations for the supercapacitor in this thesis come from an energy autonomous wireless sensor network application. The supercapacitor is designed to store harvested energy and later it powers the wireless sensor network. Materials for the supercapacitors should be chosen to be environmentally friendly and harsh chemicals be avoided. Work focuses on the sandwich structure of the supercapacitor and especially on the monolithic

approach. The aim is to use screen-printing to fabricate monolithic supercapacitor devices. As the structure has an insulative layer called a separator between the conductive electrodes, its functionality establishes the highest concern. As a result, an answer is wanted to find for the following questions.

- Can screen-printing be used to print a monolithic supercapacitor?
- How shall the separator be printed for a monolithic structure?
- How well does the screen-printed separator perform compared to the separator paper?

1.2 Structure of the thesis

After the introduction, Chapter 2 overviews the supercapacitor. Supercapacitors are compared to batteries, which are more common electrical energy storage devices. Characterization techniques used to evaluate supercapacitors are shortly described and further, different materials in supercapacitors are presented. As the supercapacitor differs from batteries some possible applications that could benefit from the supercapacitor are described. Chapter 3 focuses on the different structures of supercapacitor devices and presents additive manufacturing techniques. Also, the main topic and aims of the thesis are discussed further. Chapter 4 describes used materials and tools for supercapacitor fabrication and characterization. Chapter 5 presents and analyses the printing results of the screen-printing process and the electrical results of the fabricated supercapacitor devices. Lastly, Chapter 6 concludes the topic and results, and proposes future research directions. Furthermore, it discusses challenges that still occur on the supercapacitors with monolithic structures.

2. SUPERCAPACITOR

Capacitors are passive components in electronics with a capacity to store electrical energy in an electric field. Conventional capacitors have two electrodes separated by an insulator. Supercapacitors additionally have electrolyte between the electrodes. The interface between the electrolyte and the electrode enables higher capacitance for supercapacitors. High capacitances bear great energy density to supercapacitors together with a high power density and a long cycle life. With these attributes, supercapacitors have shown promise as electrical energy storage devices. [8]

Besides supercapacitors a more common option for electrical energy storage is batteries. Electrical energy storages have two different charge storage processes: Faradaic in the batteries, and non-Faradaic in capacitors as well as in the most supercapacitors. Real supercapacitors can have both non-Faradaic and Faradaic processes in which the latter leads to pseudocapacitance described in Chapter 2.2.2. In the Faradaic process, electron transfer takes place and produces state changes in materials. Instead in the non-Faradaic process electron transfer does not occur, but the charge is stored electrostatically. The electrostatic charge occurs when positive and negative charges are separated by a vacuum or dielectric. [8,9]

2.1 Comparison of supercapacitor and battery

Because supercapacitors and batteries have different charge storage processes it leads to some benefits over the other. The Ragone plot in Figure 1 is commonly presented to show the difference between capacitors, supercapacitors, and batteries [10]. Batteries are based on the Faradaic process which provides high energy density. However, chemical reactions of the Faradaic process are slow compared to the non-Faradaic process. Therefore, batteries have lower power density. The non-Faradaic process of the supercapacitors cannot contest batteries at energy density, but pseudocapacitance behaviours can bring supercapacitors closer to batteries on energy density. [8,10] The cycle life of supercapacitors is higher than batteries because chemical reactions occur in batteries during the charging and discharging. Some of these reactions are irreversible and will decrease active materials in batteries. [9]

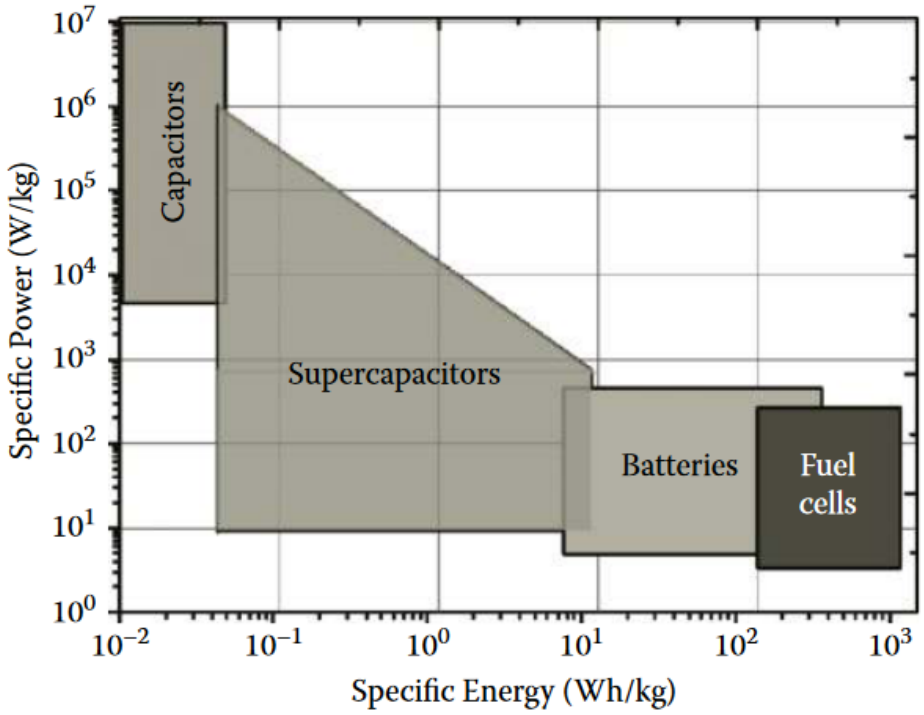

Figure 1. *Ragone plot for electrical energy storage alternatives including capacitors, supercapacitors, batteries, and fuel cells [10].*

Supercapacitors as capacitors do not have constant cell voltage, instead cell voltage will increase with charging, and decrease with discharging. However, relatively constant cell voltage can be observed with batteries during the charging and discharging as illustrated in Figure 2. [9,10]

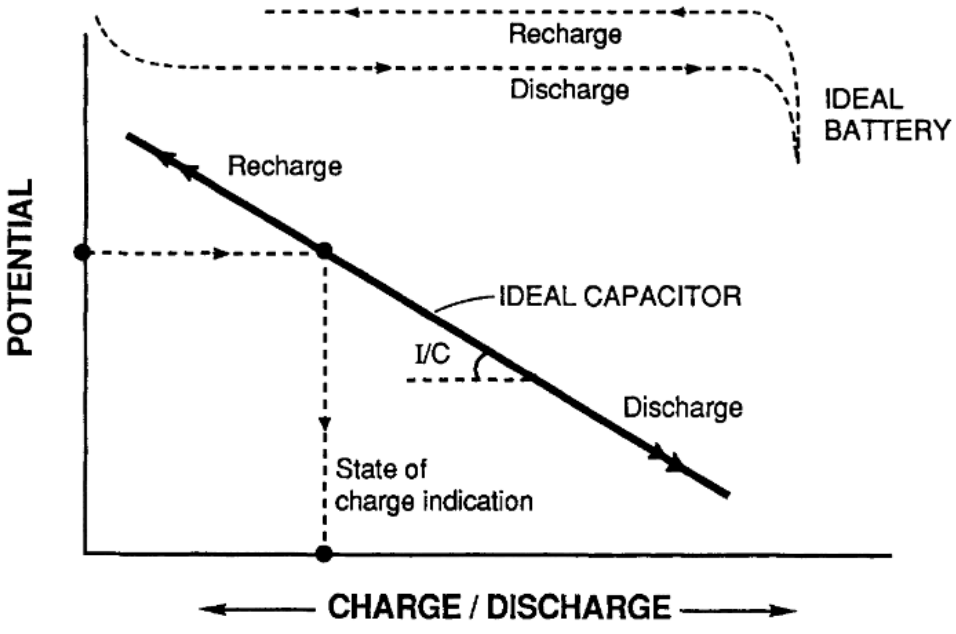

Figure 2. *Charge discharge curve of an ideal capacitor and battery. Potential as a function of the charge. [9]*

2.2 Different charge storage principles

Supercapacitors contain different charge storage principles and so supercapacitors are possible to divide into different classes. These classes are electrochemical double layer capacitors (EDLCs), pseudocapacitors, and hybrid supercapacitors. These classes are based on the different capacitive behaviours which are electric double layer and pseudocapacitance for EDLCs and pseudocapacitors, respectively. Hybrid supercapacitors are a combination of EDLCs and pseudocapacitors where the electrodes of the cell are different. One of the two electrodes in the same cell is a battery-like electrode or one from a pseudocapacitor and another electrode is a capacitor-like electrode. [8]

2.2.1 Electric double layer

When a charged object is placed in contact with an electrolyte the charged surface will attract oppositely charged ions on the surface and near it. The formation of the charged surface and ions is called an electric double layer. The simplest and earliest model to explain this behaviour of the ions and the oppositely charged surface is the Helmholtz double layer model. In the model, the plain charged electrode surface is accumulated by oppositely charged ions of the electrolyte as illustrated in Figure 3 (a). [8,9]

Later it was observed that capacitance depended on electrolyte concentration and applied voltage by Gouy and Chapman. In the Gouy-Chapman model illustrated in Figure 3 (b), the ions are point charges and do not only accumulate on the surface of the electrode, but ions diffuse into the electrolyte. The highest concentration of the opposite charges is near the surface of the electrode and concentration decreases as the distance from the surface grows. The Gouy-Chapman model predicted too high capacitance which led to the Stern model where both Helmholtz and Gouy-Chapman models are combined. In the model, ions are not point charges but have finite sizes. Therefore, ionic radius limits the smallest distance to the surface of the electrode. The surface of the electrode would be accumulated by the ions as described in the Helmholtz model and further way ions would diffuse as described in the Gouy-Chapman model. [8,9]

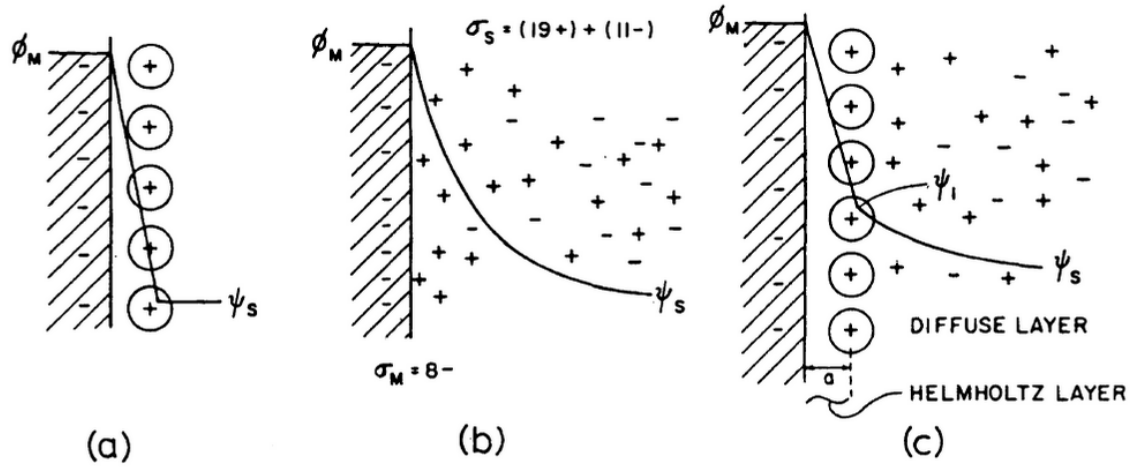

Figure 3. *Electric double layer models. (a) Helmholtz. (b) Gouy-Chapman model. (c) Stern model. [9]*

The Stern model was later improved by D.C. Grahame. Furthermore, other models were being presented in which solvents of the electrolytes have been considered. However, electric double layer models present a planar surface and therefore do not completely model phenomena in supercapacitors that have porous electrodes. It is not completely understood how the porous electrode affects the behaviour of the ions. Although pore size has shown effects on capacitance, too small pores are inaccessible to ions and therefore some areas of electrodes are unused. [8]

2.2.2 Pseudocapacitance

The electric double layer described above stores energy electrostatically, but the pseudocapacitance utilizes the Faradaic process where the charge is allowed to pass the double layer. Although supercapacitors are commonly divided into EDLCs and pseudocapacitors, it is worth emphasizing that both electrical double layer and pseudocapacitance can occur in the same electrode and electrolyte interface. Carbon-based EDLCs exhibit 1 – 5% of the total capacitance as pseudocapacitance. Conversely, batteries and pseudocapacitors exhibit some electrostatic double layer capacitance. [9]

At the electrode surface, the extent of charge acceptance (Δq) and the change of potential (ΔV) as derivative dq/dV has properties of capacitance. This capacitance behaviour is referred to as pseudocapacitance. It is separated into its own term because electrostatic capacitance differs from the origin of pseudocapacitance. [9]

2.3 Characterization of supercapacitor and key parameters

Different characterization test methods are used to measure the parameters of supercapacitors. Obtained parameters such as capacitance, resistance, and leakage current can then be used to evaluate the performance of supercapacitors. The most common tests for supercapacitors are constant current charge discharge (CCCD), cyclic voltammetry (CV), and electrochemical impedance spectroscopy (EIS). [8]

Capacitance (*C*) of a supercapacitor device is obtained from electrical charge ΔQ stored in voltage change ΔV:

$$C = \frac{\Delta Q}{\Delta V}. \quad (1)$$

The charge storage ability of the supercapacitor material can be obtained by dividing the capacitance by the mass, volume, or surface area of the electrodes. The resulting parameter is called specific capacitance (C_s). Equivalent series resistance (ESR) presents internal resistance of the supercapacitor device and is commonly got from CCCD measurement. Furthermore, leakage current parameter describes a current the supercapacitor needs to maintain the cell charge. A common way to measure the leakage current is to hold a constant voltage on a fully charged supercapacitor for several hours and measure the current flow to the cell. [11]

2.3.1 Constant current charge discharge

Constant current charge and discharge can be used to get parameters such as capacitance, and resistance. Measurement is done with controlled current, and voltage is measured over time as illustrated in Figure 4. Furthermore, charge and discharge can be cycled multiple times to measure a cyclability of supercapacitors. [8]

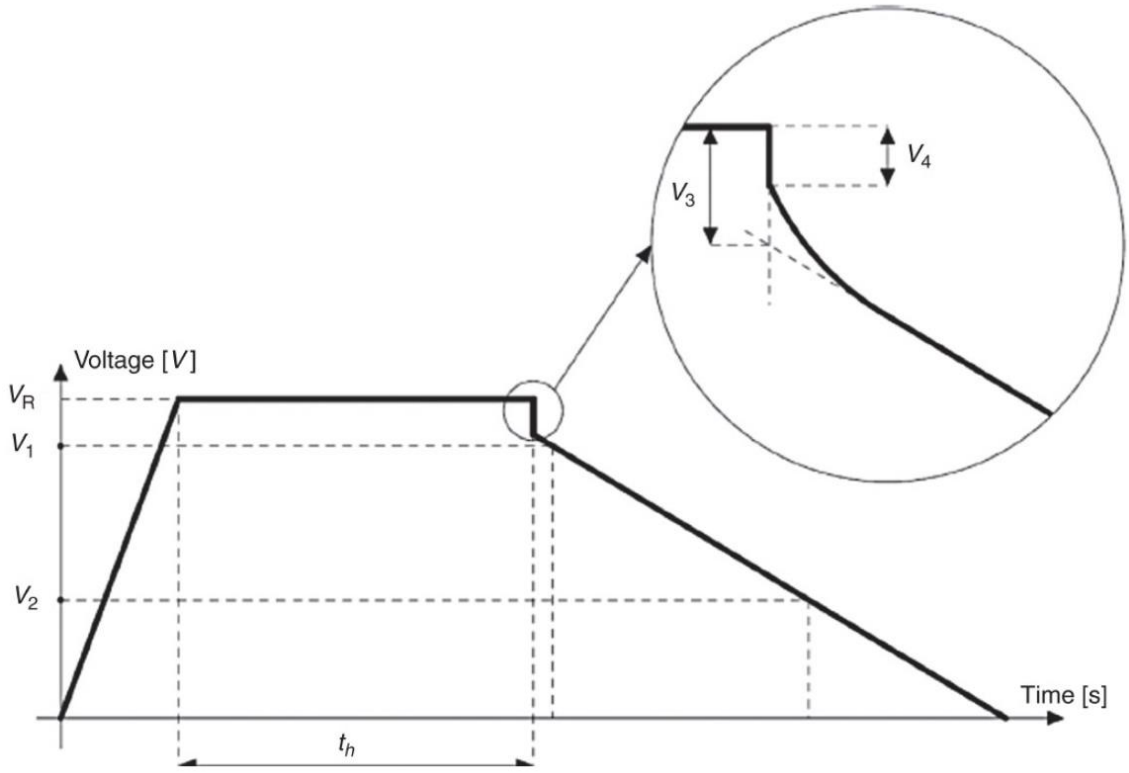

Figure 4. *Constant current charge discharge curve of a supercapacitor [8].*

Capacitance (*C*) of supercapacitors can be calculated from the discharge slope as followed:

$$C = I\frac{\Delta t}{\Delta V}, \tag{2}$$

where I is the used measurement current, Δt is the discharging time, and ΔV is the voltage drop during the discharge time. Usually, the capacitance is calculated from the voltage drop from 80% to 40% as illustrated in Figure 4 between the V_1 and V_2, rather than from the whole voltage window. In Figure 4, at the beginning of the discharge slope sudden drop of the voltage (V_4) can be found. The intersection from the start of the discharge and the auxiliary line of the discharge slope presents the greater voltage drop (V_3). ESR can be calculated from this voltage drop of V_3 and measurement current I according to the following equation: [1,8]

$$ESR = \frac{V_3}{I}. \tag{3}$$

2.3.2 Cyclic voltammetry

CV measurement is done by controlling the voltage and measuring the current. Voltage control is done by setting a speed of potential change (*mV/s*) called sweep rate, also known as scan rate. Because the current is not limited a large device can lead to high current and therefore CV is mainly considered as a laboratory test where cells are typically smaller. Together with the scan rate a voltage window is set for the measurement. The supercapacitor is first charged to the maximum voltage and after it is achieved the supercapacitor is discharged with the same scan rate. The current values of the sweeps are recorded and measurement results are usually plotted to CV-curve as current versus voltage illustrated in Figure 5. [8,11]

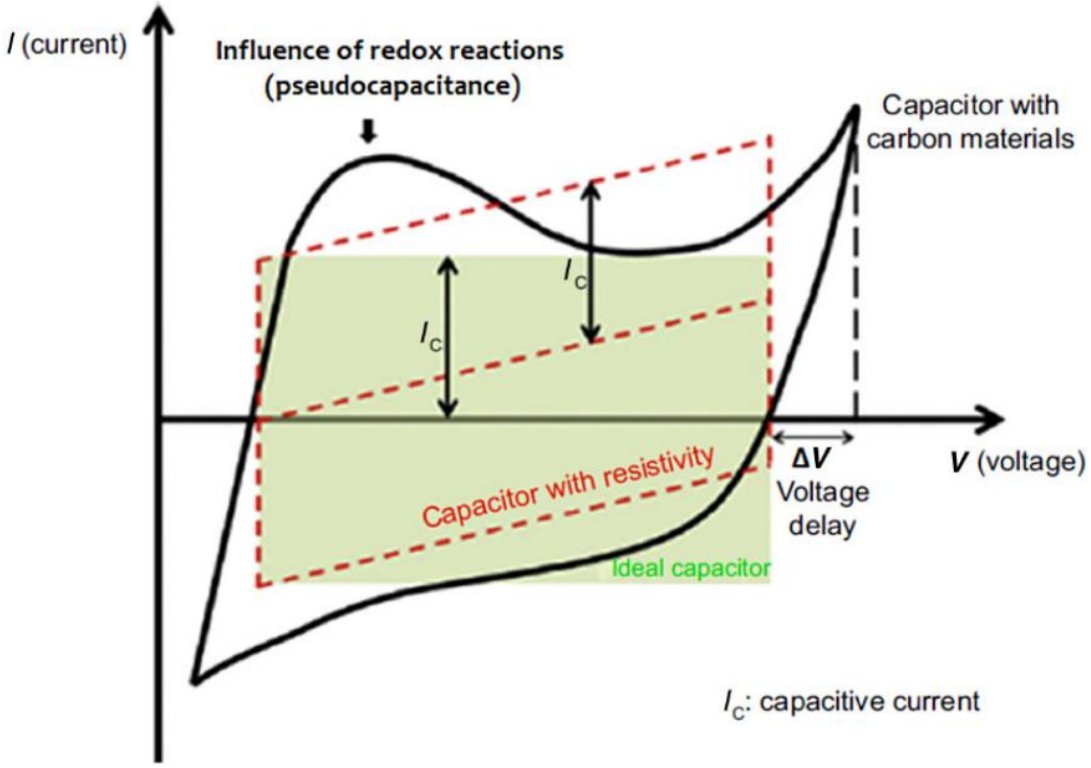

Figure 5. *Cyclic voltammetry curve of a supercapacitor [8].*

Ideal supercapacitors would create a rectangular CV-curve, but the resistivity of supercapacitors affects the shape as seen in Figure 5. Furthermore, if the supercapacitor has pseudocapacitive behaviour it can be observed as a bulge in the charging curve. [8]

2.3.3 Electrochemical impedance spectroscopy

EIS measures impedance over a range of frequencies. Measurement is done by applying a small alternative voltage (approximately 5 mV), this is done to get a linear response between the voltage and the current. Results from EIS measurements are commonly presented in Nyquist and Bode plots. The Nyquist plot shows the impedance at different

frequencies as the imaginary part versus the real part. The Bode plot shows the response between the phase angle and the frequency. [8,11] The other characteristics that EIS can provide are such as charge transfer, mass transport, charge storage process, and estimation of capacitance [11].

2.4 Supercapacitor applications

Applications options of supercapacitors can be extended if energy and power density are increased. A direct approach is to develop new materials and fabrication methods which could improve the performance of supercapacitors. [8,12] However, high power density of supercapacitors already attracts multiple applications. Applications such as transportation, power backup, and battery enhancement are discussed in the literature for supercapacitors [8,10,12].

Vehicular applications can use supercapacitors for hybrid systems where supercapacitors only provide power for acceleration and store energy during deceleration, but the main power is provided from other sources. In smart grid applications and other applications where power needs to be uninterrupted supercapacitors can be used as backup storage due to fast power output. [10] Miniaturized energy-autonomous systems are also promising applications for supercapacitors. These systems have energy harvesters to harness ambient energy for electric power. Electric power can be used directly or it is stored in supercapacitors for later use. [13]

Some applications might need higher energy or power than a single supercapacitor is able to provide. Also, the electrolyte used limits the voltage window of the supercapacitors. Therefore, modules that contain multiple supercapacitors are needed. Two options to connect supercapacitors occur and those are series and parallel. Combining series and parallel connections for supercapacitor modules desired capacitance and voltage can be obtained. [10] In series connection higher voltage can be achieved. The total voltage of the series connection (V_{tot}) can be expressed as followed:

$$V_{tot} = V_1 + V_2 + \cdots + V_n, \tag{4}$$

where V_n is the voltage of each supercapacitor in the series. In the series connection, the capacitance of each supercapacitor (C_n) forms the total capacitance (C_{tot}) by the following equation: [10]

$$\frac{1}{C_{tot}} = \frac{1}{C_1} + \frac{1}{C_2} + \cdots + \frac{1}{C_n}. \tag{5}$$

In series, a charge current between capacitors is the same but the potential differs. The voltage of cells depends on the capacitance. High voltage is generated over the cell with low capacitance and low voltage over the cell with high capacitance. Therefore, in the series connection, the voltage window of each capacitor needs to be considered and ensure that maximum voltage is not achieved. In parallel connection, total capacitance can be presented by the following equation:

$$C_{tot} = C_1 + C_2 + \cdots + C_n. \quad (6)$$

Potential difference is the same for every capacitor in parallel, but the charge between the capacitors is different. [10,14]

2.5 Structure and materials of supercapacitor

The structure of the supercapacitor and simplified DC (direct current) circuit are presented in Figure 6. In the middle of the supercapacitor is the separator. The separator divides two electrodes apart from each other and prevents short circuits. The separator is filled with the electrolyte and ions can pass through the separator layer to move between the surfaces of the electrodes. Furthermore, both electrodes are connected to their own current collectors. DC circuits illustrate two capacitances formed on the interfaces between the electrolyte and electrodes. Because supercapacitors discharge over time the leakage resistor is placed in parallel with other components. [1,10,14]

Usually, supercapacitors also have sealant for enclosing. The use of sealant depends on the cell, and it does not directly affect performance. However, without sealant supercapacitors are exposed to the surroundings and the electrolyte can leak or dry decreasing the lifetime of the cell. [10] Material requirements and some examples are given for each layer in the following subchapters. However, in common, the materials of the layers should be inexpensive, environmentally friendly, and also lightweight to keep the device weight low [14].

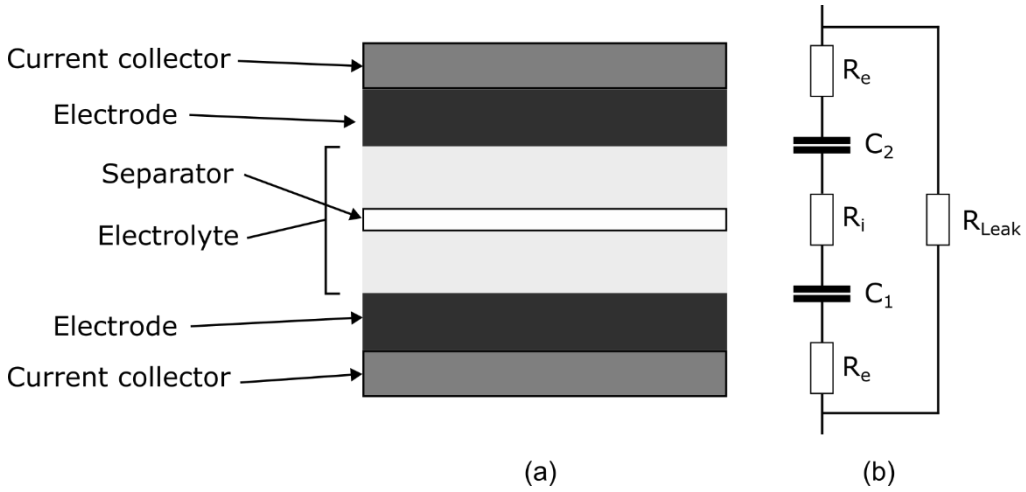

Figure 6. *Structure of a supercapacitor (a) and simplified DC circuit (b) where; R_e is electronic resistance, R_i is ionic resistance, R_{Leak} is leakage resistance, C_1 and C_2 are capacitances from electric double layer. DC circuit (b) modified from source [1].*

2.5.1 Current collector

Current collectors are used for supporting electrodes and provide a high conductive path between electrodes and external junctions. Materials used for current collectors depend on electrolyte and electrode materials. Current collectors have a significant role in the ESR of supercapacitors and therefore it is important to have high conductivity and small contact resistance with electrode materials. The electrolyte can corrode current collectors, so the material needs to be electrochemically and chemically stable against the electrolyte used. Materials should also be environmentally friendly, lightweight, and in some use cases flexible. Common materials are metals in the form of foil or foam, but also carbon-based materials are used for supercapacitors as current collectors. [3,14]

2.5.2 Electrode

Charge storage capacities and capacitances of supercapacitors are constituted by electrodes and electrolytes. Therefore, high electrical conductivity and a high specific surface area are needed from electrode materials. However, high surface areas only are not enough because supercapacitors do not benefit from all surfaces of electrodes. The high surface area is achieved with porous structures, but ions of electrolytes are not able to exploit the surface if pores are too small. It is also noticed that too big pore size will decrease capacitances. Therefore, the structure of pores is an important parameter for electrode materials and it is needed to investigate to achieve the best performance. [8,13] Other important parameters for electrode materials are chemical stability, weight, corrosion resistance, and thermal stability. [14]

Suitable electrode materials are such as carbons, metal oxides, and conductive polymers. Carbons meet the requirement of electrode materials and are common materials for EDLCs. Activated carbon is one form of carbon and is used because it is easily available and can be derived from biowaste such as coconut shells. Some other forms of carbon used are graphite, graphene, carbon nanotubes, and carbon aerogel. Metal oxides and conductive polymers have also high surface areas and are used to achieve higher energy density because these materials go through Faradaic reactions. From these two the conductive polymers have been studied more because of low cost, low ESR and easy fabrication. Common materials for conductive polymers are such as polyaniline, polypyrrole, and polythiophenes. Metal oxides such as ruthenium oxide, manganese dioxide, and tin oxide are used. [14] Both metal oxides and conductive polymers can also be used to form composites with carbon-based materials to achieve high energy density supercapacitors. [8]

2.5.3 Electrolyte

Electrolytes are generally salts dissolved in solvents, but pure liquid salts can also be used. Various electrolytes can be classified into groups such as aqueous, organic, ionic liquids, solid or semisolid, and redox-active. Each electrolyte has different attributes, but high ion conductivity and outstanding electrochemical stability are desirable. Because these have significant effects on better energy and power densities. Other requirements for electrolytes are such as a wide temperature range and chemical inertness to other materials in supercapacitors. [12,14]

Aqueous electrolytes have generally low voltage windows due to water solvents. The thermodynamic potential of the water is 1.23 V, in which the water will be electrolysed into hydrogen and oxygen. Hence generated gases can damage supercapacitors. Despite the thermodynamic potential of water, in some cases, even a 2.0 V voltage window is reported with the neutral aqueous electrolyte such as Na_2SO_4. In addition to neutral, other aqueous electrolyte types are acid and alkaline, commonly H_2SO_4 and KOH are used. These acid and alkaline electrolytes have been used to obtain higher specific capacitance compared to neutral but achieved voltage windows have been lower. [12,14]

Organic electrolytes are formed from salts dissolved in organic solvents. Organic electrolytes have typically voltage windows of 2.5 – 2.8 V, but also a wider window of 4.0 V has been demonstrated. Compared to aqueous electrolytes, achieved capacitances are low, organic electrolytes have toxic nature, and handling cannot be done in an open atmosphere. Organic electrolytes need controlled environments to avoid

water and other impurities that can produce gases and decrease the performance of the supercapacitors. [3,15]

Ionic liquid electrolytes are salts that have free or paired ions in a liquid state at room temperature. The benefit of this type of electrolyte is a high, typically 3.5 V voltage window. Furthermore, even higher operating voltages (6 V) have been shown on Pt electrodes. Some organic solvents have volatile and flammable nature and thus solvent-free ionic liquid electrolytes can have a higher temperature range and better chemical stability. However, ionic liquid electrolytes have low conductivity, high viscosity and cost compared to organic and aqueous electrolytes. [15]

Solid state or semisolid state electrolytes have low ionic conductivity, but these also fulfil the requirement of the separator. Thus, the cell can be formed without the separator layer as the electrolyte prevents the direct connection between the electrodes. Mechanical strength is high and the volume of solid or semisolid electrolytes can change which makes them good for flexible supercapacitors. The advantage of redox-active electrolytes is increased capacitances of supercapacitors, as the pseudocapacitance of supercapacitors will be contributed from both electrode materials and electrolytes. [14,15]

2.5.4 Separator

Separators in supercapacitors are required to prevent direct contact between electrodes, but let ions move from one electrode to another. Important characteristics of separators are porosity and high permeability. Separators need to uptake a lot of the electrolyte and allow ions to move easily for high ionic conductivity. If separators are not able to uptake enough electrolyte, electrodes might not have adequate ions and supercapacitors performs poorly. Thicker separators can raise ionic resistances as well as occupy larger space in supercapacitors to reduce energy density. On the other hand, the transmission distance of ions is increased with thick separators and thus can reduce the leakage current of supercapacitors. [14,16]

Good mechanical strength as well as inertness for other materials and high thermal stability is expected from separators. Materials used for separators are such as fibers and polymers of which cellulose and polyolefins are generally used in commercial products. Especially well-known paper-making process enables cost-effective cellulose separators for the supercapacitors. Additional advantages for cellulose and other biomass-based materials are renewability, degradability, and easy availability. Synthetic polymer-based separators are known to have excellent chemical stability and mechanical strength. Also, inorganic composites such as glass and ceramics can be

used as separators. These have good thermal stability and high dielectric constant. [14,16]

3. PRINTED MONOLITHIC SUPERCAPACITOR

Printed monolithic supercapacitors represent a sandwich structure, which is fabricated layer by layer. The chapter describes two different additive manufacturing methods, blade coating and screen-printing, as these are the methods used in this thesis. The first thing in the thesis work was trying to identify a screen-printing process required for the supercapacitor with a monolithic sandwich structure. Different Six Sigma tools were used to aid the design of the suitable printing process and to identify different parameters included in the process.

3.1 Fabrication techniques for printed electronics

Printed electronics is an additive manufacturing method where electronics are made by applying materials on substrates. Printed electronics is gaining awareness as it can reduce the amount of materials used as well as manufacturing is possible to complete without etching and masking. Other advantages of printed electronics are low cost, high throughput, low processing temperature, and simplicity compared to silicon-based technology. [17–19]

Printed electronics can be produced with the same printing technologies that are known in graphic arts. Printing technologies can be grouped to contact and contactless printing. Contact printing techniques are such as screen-printing, gravure printing, flexography, and offset printing. Contactless are such as inkjet printing and aerosol printing. [17] Characteristics of some printing techniques are compared in Table 1. Also, coating techniques such as doctor blade coating, casting, and spin coating can be used as additive manufacturing methods. Many printing and coating techniques can also be done as a roll-to-roll (R2R) process. In the R2R process, substrates are unwound from a roll for different treatments and then rewound on another roll. [20]

Table 1. Printing technique comparison [17,18].

Technique	**Maximum solid loading (%)**	**Ink viscosity (Pas)**	**Maximum particle size (µm)**	**Layer thick-ness (µm)**
Screen	90	0.1 – 1000	1/10th of mesh opening	0.015 – 100
Gravure	30	0.01 – 1.1	15	0.1 – 8
Flexography	40	0.01 – 2	15	0.04 – 2.5
Inkjet	20	0.001 – 0.05	1/10th of nozzle diameter	0.05 – 20
Offset	90	20 – 100	10	0.5 – 200

3.1.1 Doctor blade coating

Doctor blade coating is a simple film coating technique where a blade is moved over a coated sample. The blade moves linearly across the sample and covers it with a coating solution which was placed in front of the blade as seen in Figure 7. A fixed distance between the sample and the blade is a simple way to define the thickness of the coated film. Another benefit of this technique is minimal coating solution loss. At first, it is hard to estimate the proper amount of coating solution but after optimizing the process, less than 5% coating solution loss can be achieved. [20]

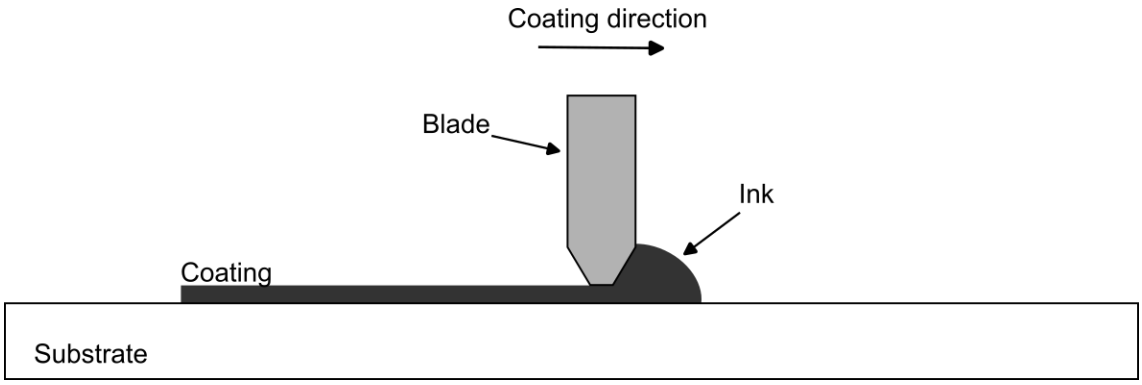

Figure 7. *Doctor blade coating technique.*

3.1.2 Screen-printing

Screen-printing is illustrated in Figure 8, it is a simple printing technique where inks are pushed on substrates through screens. The screen has a mesh that is covered with emulsion and is fixed to the frame under tension. Printing patterns on the screen are parts without the emulsion and thus ink gets through the mesh on specific areas. The ink is applied on the screen where a squeegee is pressed down and moved linearly across the screen. The squeegee forces the ink through the open areas of the mesh on the substrate. [20]

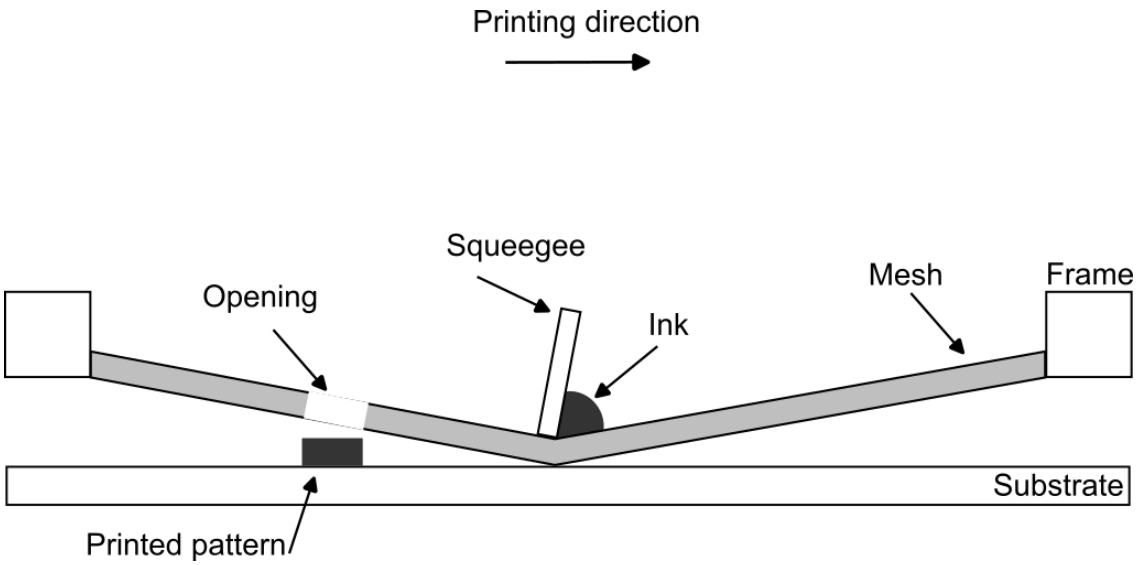

Figure 8. *Screen-printing technique.*

While traditionally screen-printing is a flatbed process it can also be done from R2R. In the R2R process the screen is shaped as a cylinder and the squeegee is placed inside the cylinder with the ink. The substrate is then fed between two rolls where one is for support and another is the screen. [20]

3.2 Different structures of supercapacitor cell

Printed supercapacitor cells can be arranged in different structures such as sandwich and planar interdigitated illustrated in Figure 9. In a sandwich structure, current collectors, electrodes, separator, and electrolyte layers are stacked on top of each other. On the other hand, in the planar structure layers are basically on the same level. The planar structure can be implemented with interdigitated electrodes. As electrodes are not overlapping and are separated by narrow gaps, the need for the separator is eliminated. Therefore electrolytes can be applied directly on top of electrodes and not to the separator. [21]

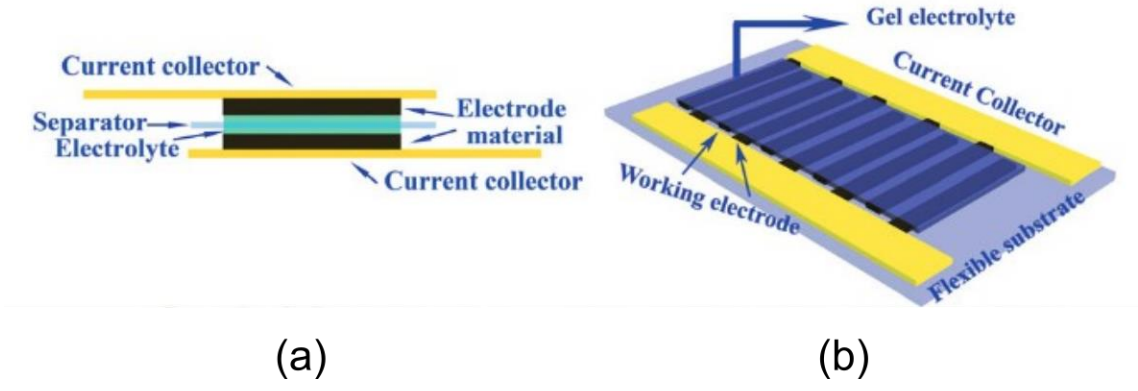

Figure 9. *Sandwich (a) and planar structure (b) of the supercapacitor cell [21].*

Typically sandwich structures are fabricated from two separate electrodes that are later assembled with the separator and electrolyte creating a face-to-face (F2F) structure illustrated in Figure 10 (a). In the assembly, the electrodes are soaked with electrolyte and the separator is applied on one electrode. Then the other electrode is aligned on top of the separator in a way that the electrodes fully overlap. [7] The planar structure has a simpler fabrication process as the layers are on one thin plane and additionally thin structure benefits flexibility. The use of screen-printing is demonstrated with interdigitated supercapacitor where only electrodes are printed on the substrate and after drying gel electrolyte is applied. [22]

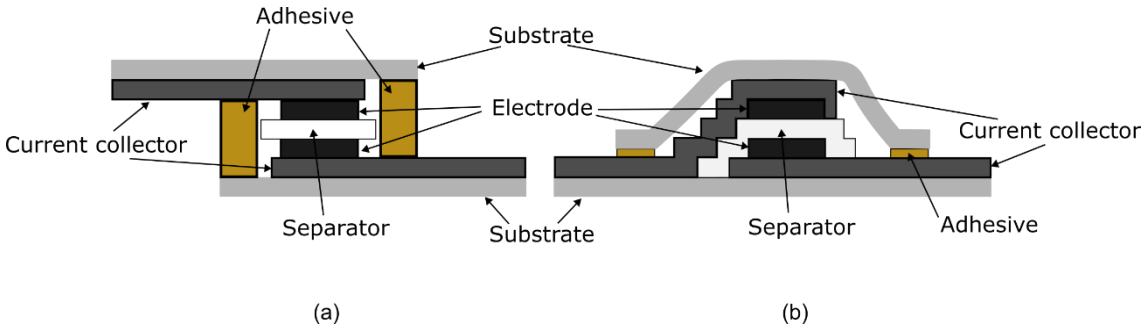

Figure 10. *Face-to-face structure (a). Monolithic structure (b).*

In a monolithic structure, layers are overlapping as normally in the sandwich structure as illustrated in Figure 10 (b). The monolithic stack is fabricated by printing layers on top of each other which eliminates the assembly step normally in the F2F sandwich structure. Although the assembly step is eliminated, the monolithic structure requires multiple prints to create all layers compared with the planar structure. On the other hand, the ESR tends to be higher for planar interdigitated structures as the current collectors are longer and narrower than in sandwich structures. [7,22]

3.3 Fabrication of monolithic structure

The motivation for the monolithic structure is a simpler fabrication process as the assembly step is eliminated. As layers are printed on top of each other, the fabrication of the whole structure should be possible with the screen-printing. Screen-printing enables high-volume production even in the R2R fashion at a low cost. The supposed screen-printing process for the monolithic supercapacitor follows the steps illustrated in Figure 11. Each layer is printed once, dried, and then the next layer is printed on top of the previously cured layer.

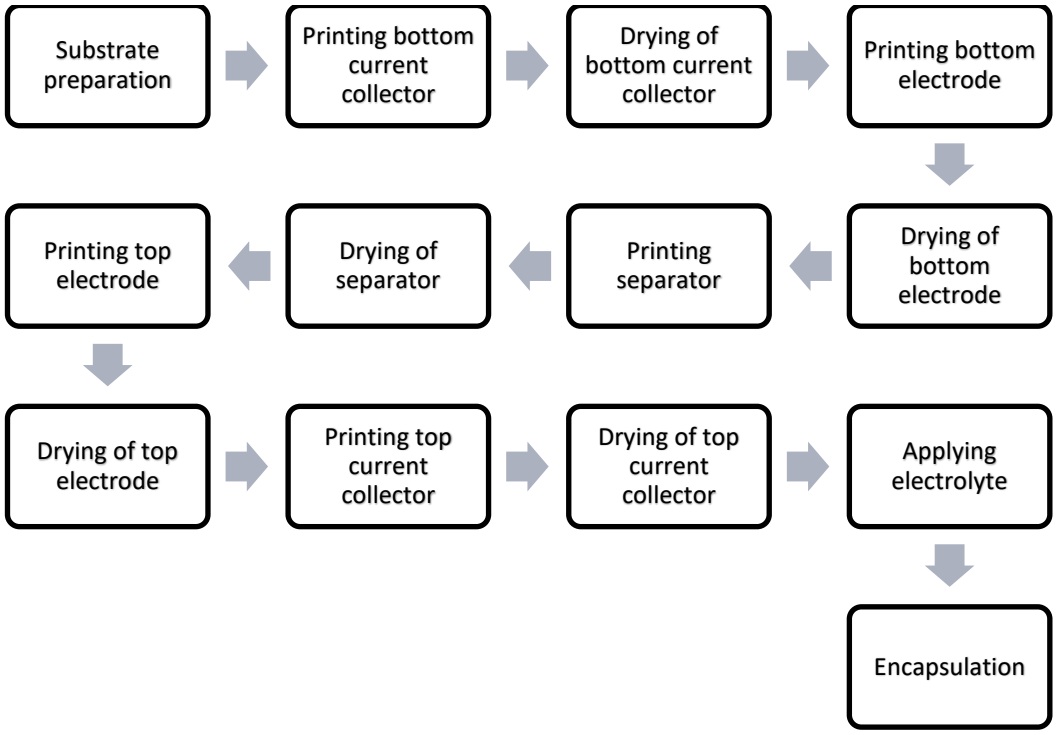

Figure 11. *Supposed screen-printing process for monolithic supercapacitor.*

SIPOC (Suppliers, Inputs, Process, Outputs, and Customers) diagram and Cause and Effect matrix (C&E matrix) tools are used to understand the fabrication process better and to identify the most important factors. One challenge for the screen-printing process is the preparation of suitable inks. Inks should be compatible with the screen-printing technique, but also compatible together. As the structure is made layer by layer the inks should have good adhesion as well as wettability properties to adjacent layers. [6,7,19] Another challenge in the process is the separator layer as it needs to prevent contact between the bottom and top layers but allow the ions to pass through it. A risk in the process is that in the upper layers, especially the top electrode, the ink could leak through the separator layer. Furthermore, force is applied on the squeegee which presses down the previous layers. Force should be moderated so that layers are not crushed, and the porosity of the layers is retained. Therefore, the overall performance of the supercapacitor does not decrease. Other printing parameters such as snap-off and squeegee speed have shown to affect prints. However, prediction for optimal settings may be hard as these parameters depend on ink properties. [23]

In this thesis, the main purpose is to be able to fabricate the monolithic supercapacitor with screen-printing. In the structure the weak link is expected to be the separator and therefore more focus has been placed on the separator than the other layers. The C&E matrix indicates that the most significant effect in the process would come from the inks and the screens. In the thesis the different key parameters in the screen-printing as well

the main factors were wanted to identify to improve the process. If the supposed screen-printing process of the monolithic supercapacitor is successful, the supercapacitor module was also intended to be fabricated as the supercapacitor applications may require combinations of several cells.

4. RESEARCH METHODOLOGY AND MATERIALS

In this thesis selected materials for the supercapacitors were desired to be non-toxic, sustainable, and easily available. Activated carbon (AC) was used for electrodes and the separator layer was made from talc and cellulose. Both layers had chitosan as the binder and harmful solvents were avoided. Aqueous electrolytes were chosen for use as they are easy to handle and have lower environmental effects compared to organic electrolytes. [14].

Blade coating and screen-printing were two fabrication techniques used. Blade coating was used for F2F and monolithic supercapacitors. Screen-printing was used for monolithic supercapacitors with one cell and modules having three cells in series. In the chapter, the difference between each sample is described, as well as used fabrication and characterization methods are introduced.

4.1 Materials for supercapacitors

Supercapacitors were printed on a laminate of aluminium and polyethylene terephthalate (PET) made by Pyroll. The thicknesses of aluminium and PET are 9 µm and 50 µm, respectively. Current collectors were printed with commercial graphite ink Loctite EDAG PF 407C E&C. Electrode and separator inks were self-made and the preparation of those are explained in the chapter below.

Instead of separator ink, a paper sheet with a thickness of 20 – 30 µm from Glatfelter was used as the separator for the F2F structures. The electrolyte used for all supercapacitors was sodium chloride dissolved in deionized (DI) water in a mass ratio of 1:5. Encapsulations of the monolithic supercapacitors were done using the same Al/PET laminate that was used as substrate. Supercapacitor samples were sealed with 3M 468MP 200MP adhesive tape.

Both the electrode ink and the separator ink used the same chitosan binder which was prepared in a glass bottle on a magnetic stirrer. Before the bottle was placed on the magnetic stirrer, it was filled with 67 g of DI water and 0.7 g of acetic acid. This acid solution was stirred at high rpm (revolutions per minute) and 1.7 g of chitosan powder (Sigma-Aldrich Chitosan from shrimp shells) was slowly poured into it. The mixture has been kept on the stirrer until a homogeneous solution was achieved.

The electrode ink was prepared in a plastic bag where the ink was mixed manually. The electrode ink contained 6.94 g of chitosan binder solution, 3.09 g of AC (Kuraray YP-80F), and 2 g of DI water. Chitosan binder, AC, and DI water were mixed in the plastic bag, and it was continued to be squeezed manually until agglomerates disappeared. The separator ink contained chitosan binder, talc (Finntalc M15E from Elementis), cellulose (Sigma-Aldrich Cellulose fibers), and DI water. For separator ink, 6.94 g of chitosan binder solution, 3.4 g of talc, and 0.85 g of cellulose fibers were mixed in a plastic bag in the same way as the electrode ink.

4.2 Dimensions and screens used for supercapacitors

Different screens were used for the fabrication of monolithic supercapacitors and are presented with characteristics in Table 2. Screen NBC EX 24-125 for the electrodes and NBC EX 12-150 for the separator were missing a three-cell module pattern. All other screens had patterns for single-cell and three-cell supercapacitor modules.

Table 2. Screens that are used for screen-printed supercapacitors.

Layers	**Screen**	**Mesh count (/cm)**	**Thread diameter (µm)**	**Mesh opening (µm)**	**Open area (%)**
Separator, Current collectors, Electrodes	NBC EX 24-125	24	125	298	50
Separator	NBC EX 12-150	12	150	696	68
Separator	NBC EX 31-071	31	71	246	60
Electrodes	Saatilene Hi-Dro 48-055W	48	55	153	55

The lateral dimensions of the monolithic supercapacitors are presented in Table 3. The margins between the layers for blade coating were higher than for screen-printing because the used blade coating process was not as accurate as the screen-printing method. Blade coating was also used for the F2F supercapacitors, and thus one electrode has a dimension of 32 mm x 10 mm and the other has 22 mm x 10 mm to facilitate direct comparison between the fabrication methods. Both electrodes were on top of current collectors with dimensions of 34 mm x 31 mm.

Table 3. Height and width of each single-cell supercapacitor layer.

Layer	Dimensions of blade coated supercapacitor (mm x mm)	Dimensions of screen-printed supercapacitor (mm x mm)
Bottom current collector	34 x 31	34 x 31
Bottom electrode	32 x 10	33 x 10
Separator	26 x 16	31 x 14
Top electrode	22 x 10	29 x 10
Top current collector	18 x 31	27 x 30

The screen-printed single-cell monolithic supercapacitor is illustrated in Figure 12 together with a three-cell monolithic supercapacitor module. Printings were carried out in the direction showed in Figure 12 for all screen-printed samples as well as for blade coated samples. In the module, the electrodes have a width of 1.5 mm, and the widths of the other layers are minimized so that the gaps between the separators are 10 mm.

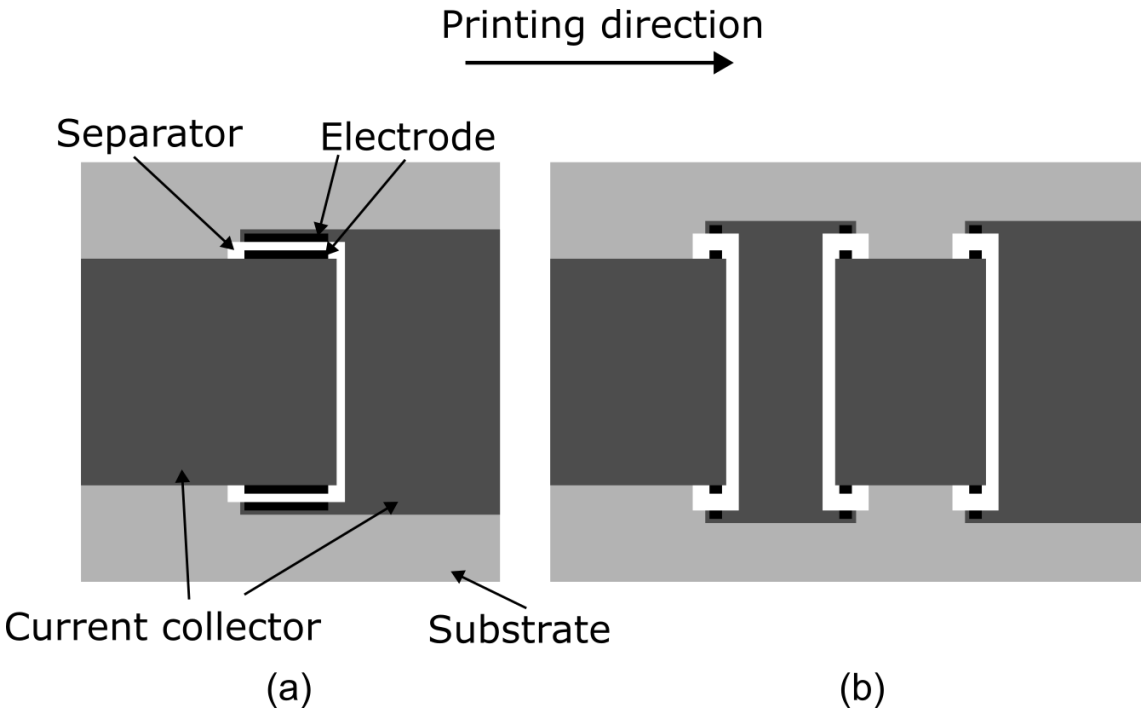

Figure 12. *Top views of screen-printed supercapacitors without encapsulation. (a), Single-cell monolithic supercapacitor. (b), Three-cell monolithic supercapacitor module.*

4.3 Supercapacitor fabrication process

The fabrication process of the monolithic supercapacitor for blade coating and screen-printing followed the same steps. The fabrication process started by printing a bottom current collector on the PET side of the substrate. The second layer was a bottom electrode which came on top of the bottom current collector. The third layer was a separator which was printed on top of the bottom electrode. The fourth layer on top of the separator was a top electrode, and the uppermost printed layer was a top current collector. Before a new layer was printed the previous layer had to be cured in an oven.

The current collectors were cured at 95 °C for 1 h, and the electrodes as well as the separator were cured at 60 °C for 30 min.

The separator was printed only once in the initial process flow but was later observed that a single print did not create a uniform layer. Without the uniform layer, the separator is not able to prevent contact between the electrodes. Therefore, the effects of multiple prints of the separator layer were investigated. The results of different separator layer prints are presented in Chapter 5. In the blade coating the uniform separator was achieved with one coating but was coated twice, and then cured, to ensure even layer formation. In the F2F structure, the separator was not printed and therefore both electrodes were printed directly on separate current collector layers.

4.3.1 Blade coating process

In the blade coating, the blade was placed to move on the mask as seen in Figure 13. This way the thickness of the substrate was left away from the total gap size. The total gap size was defined together with the thickness of the mask and the gap of the blade. The gap for the blade was set on a glass platform of the blade coating machine with a feeler gauge. Gap sizes used for different layers are presented in Table 4.

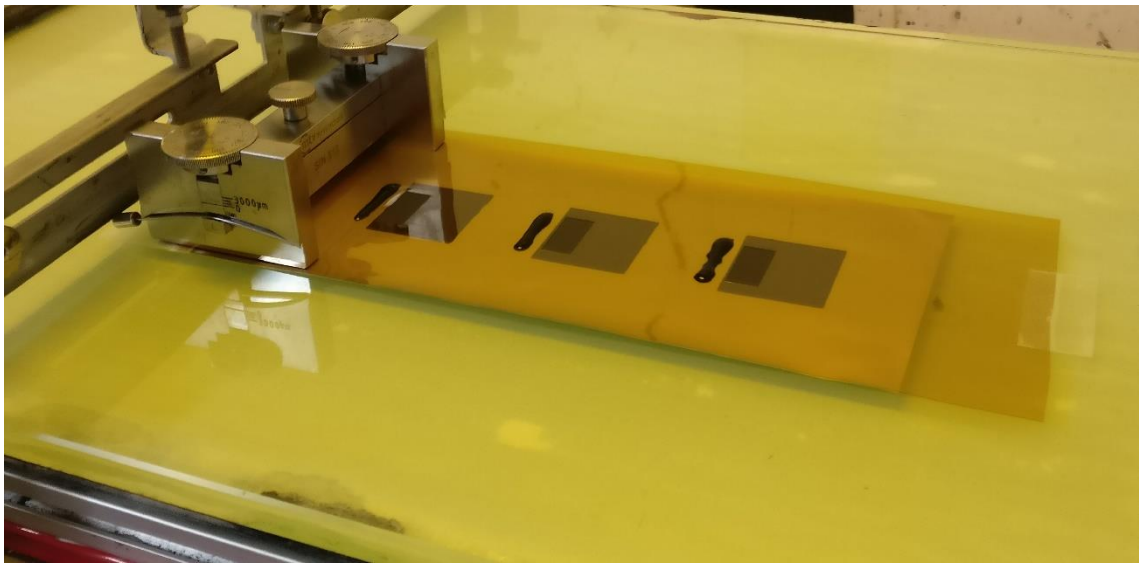

Figure 13. *Blade coating set-up for electrode coating.*

Table 4. Gap size for each supercapacitor layer.

Layer	Gap size (mask + gap of the blade) (µm)
Bottom current collector	100 (50 + 50)
Bottom electrode	100 (100 + 0)
Separator	300 (50 + 250)
Top electrode	100 (100 + 0)
Top current collector	150 (50 + 100)

The mask used during the blade coating process was a patterned polyimide film with a thickness either of 50 µm or 100 µm. The mask was visually and roughly aligned with the substrate and together placed on the glass platform. Both the mask and the substrate were then taped on the glass platform to prevent movement of the mask and the substrate. For every layer, the ink was applied on the mask in front of the patterns that needed to be coated. The blade was then driven over the substrate and the mask roughly at a speed of 6 mm/s. After coating the mask was peeled off from the substrate and the sample was cured in the oven. Other layers were coated once, but the thicker separator layer was coated twice before curing to achieve a better layer. For the separator layer, after the first coating, the blade was moved back to the start position and then the second coating was carried out with the same mask.

4.3.2 Screen-printing process

Fabrication of a monolithic supercapacitor was made by using the Ekra X5 Professional screen-printer presented in Figure 14. In the printer, ink was first spread on a screen with a metal squeegee that moves in the reverse direction. Next, the rubber printing squeegee moved forward and prints the ink on the substrate through the screen. The substrate was transferred into the screen-printer with a vacuum table. The vacuum held the substrate in place and prevented movement of the substrate during the printing. However, under the screen, the screen-printer was able to move the whole vacuum table which enabled alignment for the printing process.

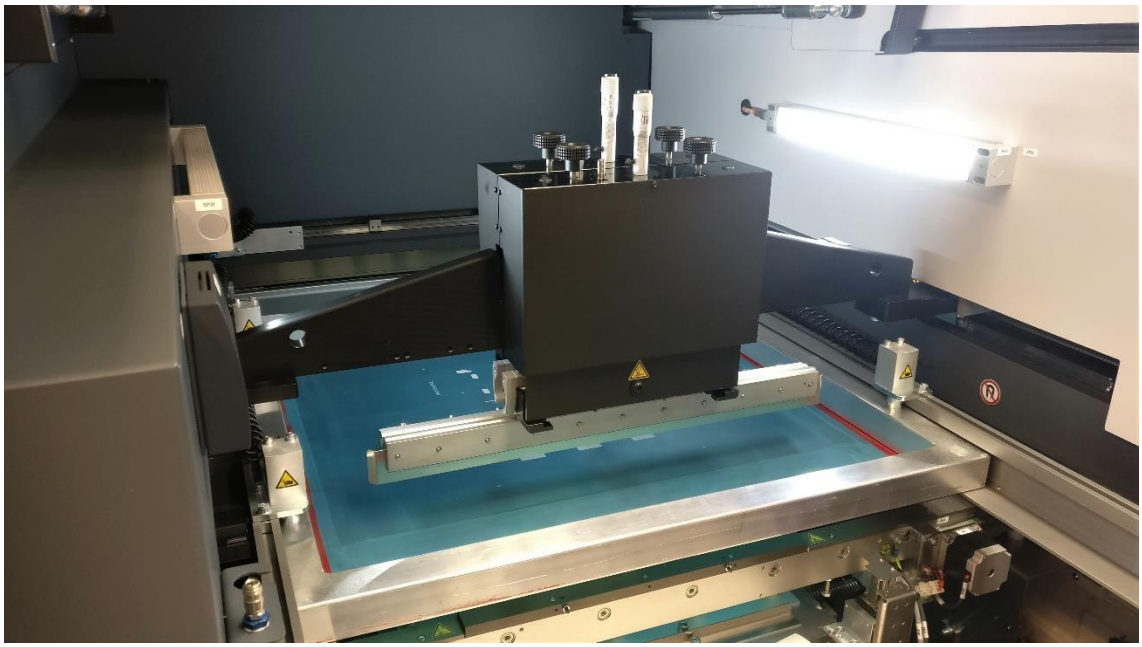

Figure 14. *Screen-printing machine Ekra X5 Professional.*

The vacuum table was bigger than used substrate sheets and therefore polyimide film was used to cover the rest of the table. Polyimide cover was also used for alignment as the alignment patterns were located mainly at the side of the screen and the substrate of the size of one supercapacitor did not overlap those. All single-cell supercapacitors were aligned with the polyimide cover, and the cover was later aligned with the screen. For the three-cell supercapacitor module, alignment patterns were printed on the substrate with the bottom current collector. Alignment patterns were then used to align the screen and the substrate when the upper layers were printed. The printing squeegee had a 60° angle, and the same squeegee was kept for all prints even though some wear was observed. All the layers of the supercapacitors were printed at the beginning with the initial printing settings that are presented in Table 5.

Table 5. Initial settings for printing parameters in the Ekra X5 Professional

Printing speed forward (mm/s)	**Printing pressure forward (N)**	**Snapp off (mm)**	**Printing speed reversed (mm/s)**	**Printing pressure reversed (N)**
20	200	2.00	40	100

Printing was started from the current collector with screen NBC EX 24-125. The electrode was printed on top of the current collector with screen NBC EX 24-125 for the single-cell monolithic supercapacitors and with screen Saatilene Hi-Dro 48-055W for the monolithic supercapacitor modules. For the separator layer, all available screens were tested to find the most suitable one.

4.3.3 Finalization of supercapacitor fabrication

Both fabrication methods produce samples that still needed the electrolyte and encapsulation. The monolithic samples were tested with a digital multimeter before being saturated with the electrolyte. When dry, a successful sample should have high resistance between the current collectors. If the measured resistance is low, on the order of hundred ohms, the separator does not prevent a short circuit. With low resistance (a couple of kilo ohms or below) the supercapacitor could still pass the electrical characterization test, but the leakage current would be too high. This would lead to quick discharge, and hence the supercapacitor would not be practical.

The encapsulation of the monolithic supercapacitor is illustrated in Figure 15. First, the adhesive tape was placed around the separator. A pipette was used to transfer the electrolyte to the separator from its edges until it was saturated. Lastly, the release paper of the tape was removed, and a piece of the Al/PET laminate was placed on its PET side down. Because the module had three cells the tape was placed around all separators as illustrated in Figure 16.

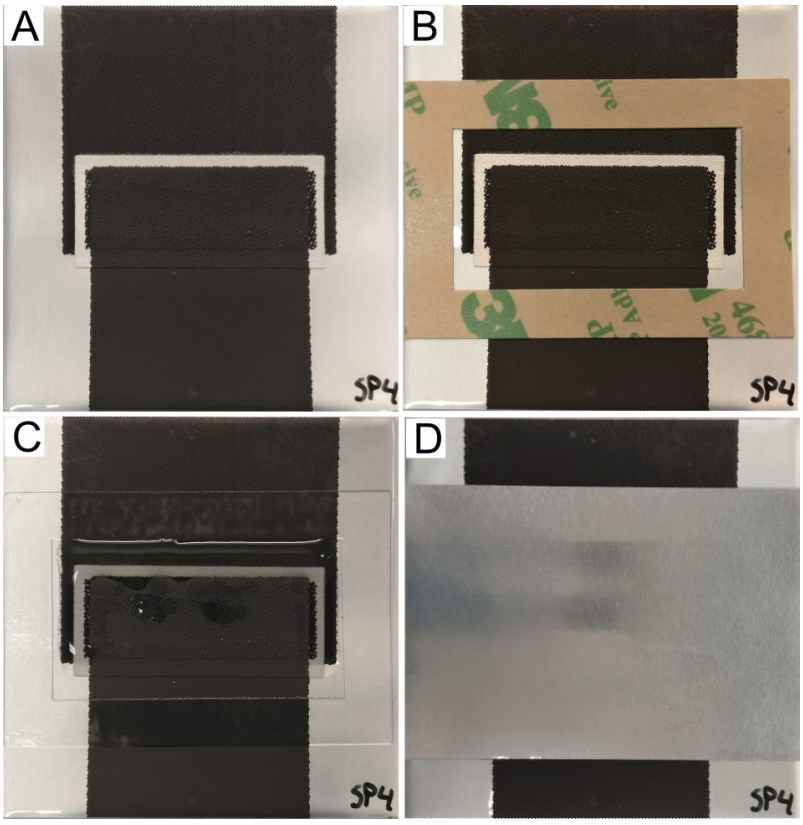

Figure 15. *Monolithic supercapacitor. A, Printed structure. B, Tape around the separator. C, Electrolyte added to supercapacitor. D, Encapsulated supercapacitor.*

Figure 16. *Adhesive tape on monolithic three-cell supercapacitor module.*

The F2F supercapacitor is assembled from two substrates that both have a current collector and electrode printed on, as illustrated in Figure 17. First, the adhesive taper is placed on one half. A pipette is used to transfer electrolyte to both electrodes and after this paper separator is placed on one electrode in a way that the tape is around it. More electrolyte is added on the separator until it is saturated. The release paper of the tape is removed and the electrode without the paper separator is turned on top of the other in a way that the electrodes are face to face.

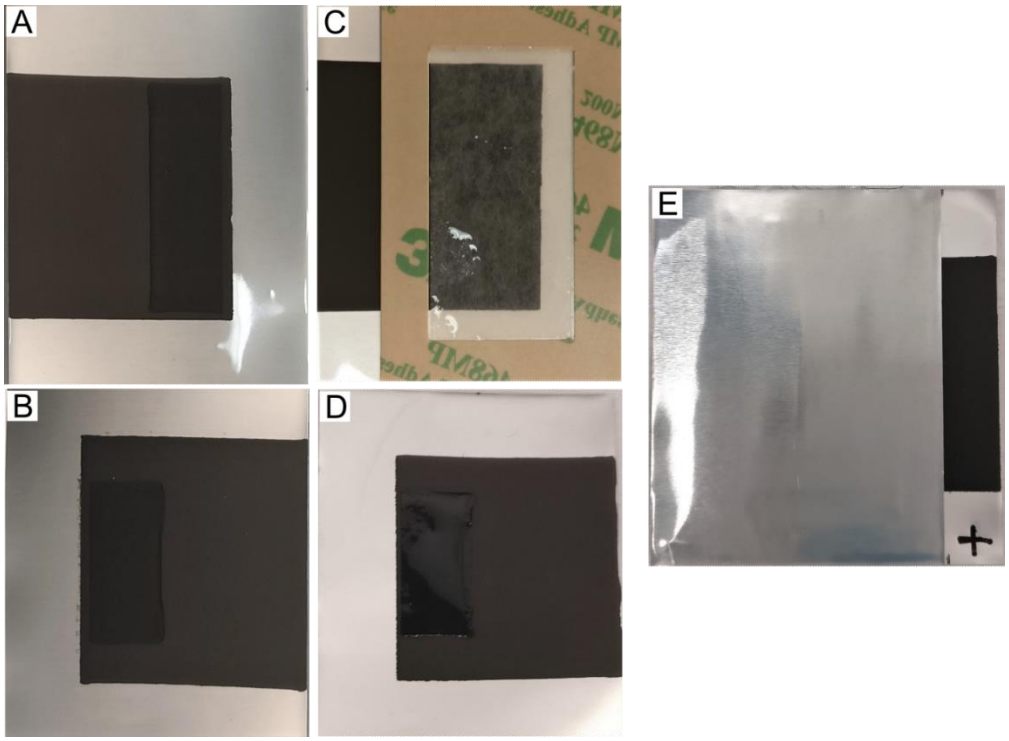

Figure 17. *Face-to-face structure. A, Bottom half. B, Top half. C, Bottom half with electrolyte, tape, and separator. D, Top half with electrolyte. E, Two half combined.*

4.4 Characterization tests

Supercapacitors and different printed layers in it were characterized and results were compared with each other. Before the electrolyte was applied, the short circuit of the supercapacitors was tested with a digital multimeter. All samples with dry resistance under 3.5 kΩ were considered short-circuited and only samples over 3.5 kΩ were further characterized electrically.

The quality of the printed layers was viewed with a microscope and a stylus profilometer. After a layer was printed it was checked with bare eyes, but more accurately the layers were viewed with Olympus BX60M microscope and Olympus SZX9 stereo microscope. Microscopes were equipped with an Olympus SC50 camera which was used to capture images of the layers.

4.4.1 Electrical characterization

Electrical characterization of the supercapacitors was tested with a Maccor 4300 test station which had several channels to test multiple samples simultaneously. The test station was programmed to perform several charge and discharge steps in series with different constant currents. After the constant current measurements, the samples were also run with different scan rates for CV measurement.

The test program started with capacitance and ESR measurements. The supercapacitors were first charged with constant current to the desired voltage and kept at it for 30 min. After that supercapacitors were completely discharged with the constant current. At the beginning of the discharge, the voltage drop was observed and the ESR was calculated from it with Equation 3. The capacitance was calculated with Equation 2 from discharge, where the voltage was between 80% and 40% of the original voltage. Next, the supercapacitor was charged and held for 1 h at the desired voltage. The presented leakage current was the current that was needed to hold the applied voltage at the end of the 1 h charge.

4.4.2 Surface profile and roughness

DektakXT Stylus Profiler was used to measure the surface of the printed layers. The device was equipped with a ceramic vacuum sample fixture and a stylus with a radius of 2 µm. Stylus force was 5 mg for all measurements. Measurement data was plotted to graph but also used to calculate roughness parameters arithmetic average (R_a) and root mean square (RMS) with the following formulas:

$$R_a = \frac{1}{N}\int_0^N |z - m|\, dx, \tag{7}$$

$$RMS = \sqrt{\frac{1}{N}\int_0^N z^2\, dx}\,, \tag{8}$$

N is a sample size, *z* is a measured height from a reference line, and *m* is a mean of *z* [24].

4.5 Surface treatment

Surface treatment with plasma and ultraviolet-ozone (UV-ozone) can be performed on the substrate and on all printed layers to improve the wetting of the ink. However, surface treatments were used only for screen-printed samples. Diener Atto was used for plasma treatment and available gases were oxygen (O_2) and nitrogen (N_2). The treated sample was placed in a vacuum chamber where the plasma was generated under low pressure recommended by the manufacturer.

Novascan PSD-UV was used for UV-ozone surface treatment. The sample was covered with a casing, in which ultraviolet light was produced. Light increases the energy of organic molecules, and the presence of oxygen produces ozone. The combined effect of the treatment will be effective for the destruction of an organic material. [25]

5. RESULTS AND ANALYSIS

Any of the inks were not previously screen-printed with the Ekra X5 and thus it was unclear how those materials will behave in the screen-printer. However, current collector and electrode inks have been used previously in the blade coating, but the separator ink was recently developed in the InComEss project. Hence, the compatibility of inks and fabrication methods was tested at the beginning. The chapter demonstrates the required modifications of inks for successful printing and discovers the effects of different fabrication parameters. In more detail, different screen-printed separator layers are evaluated and compared. Finally, the performances of the monolithic supercapacitors that are fabricated with the discovered process are presented.

5.1 Printability of the inks for supercapacitors

The first ink to screen-print was the graphite ink for the current collectors. The screen NBC EX 24-125 worked well with graphite ink and printing did not cause problems. Only if the ink was not stirred properly, the ink spread poorly on the screen at the beginning. Single print with the initial printing settings produced a uniform layer.

Electrode ink was tested on top of the screen-printed graphite current collector. Screen-printing of the electrode ink was problematic. On the first run, the ink clogged the openings of the screen and dried on the squeegee as seen in Figure 18. Separator ink was tested on a sample where the current collector and the electrode were already screen-printed. The separator ink did not clog the screen, but the print did not create a uniform layer. Additionally, the ink did accumulate on the squeegee and dried on it as the electrode ink did.

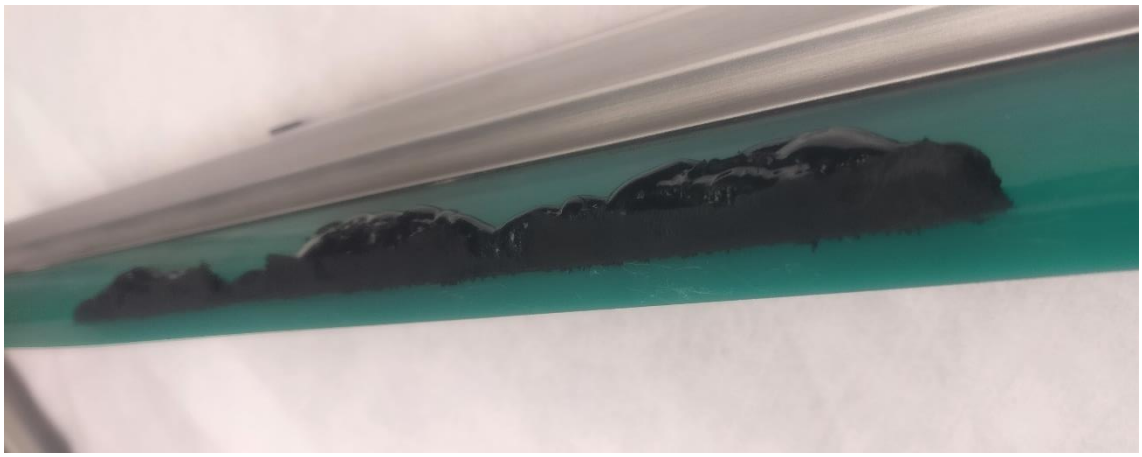

Figure 18. *Dried electrode ink accumulated on the printing squeegee.*

The screen-printer was being equipped with a sensor which can be used to monitor temperature and humidity during the printing sessions. Inks were tested to print at different times when the room conditions were different. The temperature was constantly around 21 °C, but humidity varied between 6 and 40%. However, the humidity was not observed to have an obvious effect on printing quality. Especially with electrode ink, the clogging behaviour did not change. Also, with the other inks produced prints were similar regardless of humidity.

5.1.1 Electrode

The electrode ink described in Chapter 4.1 was tested in the screen-printing process, but this ink dried too quickly and clogged the opening of the screen. Therefore, a drying retarder was needed for the ink to prevent clogging. Commercial TEXILAC RITARDANTE from Eptainks was added to ink with different weight percentages (wt%) of 9.5, 14.9 and 25. The low amount of Texilac mostly prevented clogging, but the ink still accumulated on the squeegee and eventually dried. With a 25 wt% the ink did not accumulate heavily on the squeegee and multiple samples were possible to print without the clogging. Hence, the new electrode ink contained 6.94 g of chitosan binder solution, 3.09 g of AC, 2 g of DI water, and 4.01 g of Texilac. As earlier the chitosan binder solution, AC, and DI water were first mixed to create a paste and after that, the Texilac was added. All materials were mixed by squeezing in the plastic bag until agglomerates disappeared.

Table 6. Optimized printing parameters for electrode ink.

Printing speed forward (mm/s)	Printing pressure forward (N)	Snapp off (mm)	Printing speed reversed (mm/s)	Printing pressure reversed (N)
10	200	2.00	40	100

The new electrode ink was suitable for multiple prints in screen-printing, but after 20 minutes of printing the ink started to clog the screen. It was later observed that solvent is a critical part of this electrode ink, and a higher solvent share could have improved the printing more. Furthermore, the electrode ink has a relatively short shelf life. Because the use of ink stored for a couple of weeks caused clogging of the screen. The clogging with the stored ink was avoided by adding DI water to the ink. Added solvent lowered viscosity and slightly increased the wettability of the electrode ink.

From printing parameters, the printing speed forward seemed to have the most significant effect on uniform print. Surface treatment has a similar effect as printing speed. Plasma and UV-ozone both improved prints to a more uniform layer. From different surface treatment options, 30 min nitrogen gas plasma was chosen to use for

practical reasons. However, after surface treatment the mass of current collectors decreased and therefore parameters need optimizing in future work. For example, with a shorter treatment time, the plasma might have a smaller effect on bonds between the carbons. Thus, effects on the surface may be reduced and material loss be avoided. But the mass loss could also come from impurities cleaned away in the treatment.

5.1.2 Separator

As well as the electrode ink, the separator ink described in Chapter 4.1 was tested in the screen-printing process. Separator ink did accumulate on the squeegee but did not clog the screen. Another problem with the separator ink was poor wetting as single print did not cover the desired area fully. Because there was no issue with clogging only DI water was added to improve the printing. Three different ink versions were tested: 1 g, 2 g, and 3 g of DI water were added to the separator ink described in Chapter 4.1. The separator ink with 2 g of DI water was enough to prevent the ink from accumulating on the squeegee and it also improved the wetting, although coverage was incomplete. In the separator ink, 3 g of additional DI water decreased viscosity more but did not significantly improve printing compared with 2 g of DI water. As the mesh openings in the screen were big and low viscosity ink can flow through it, the 2 g additional water was chosen to use in the separator ink for supercapacitors.

Separator ink for screen-printing was prepared with additional water, and thus new recipe is 6.94 g of chitosan binder solution, 3.4 g of talc, 0.85 g of cellulose fibers, and 2 g of DI water. All materials are mixed in a plastic bag. In addition to that the bag is placed in a sonication bath for 30 min to help avoid agglomerates. For blade coating the separator ink is still prepared as in Chapter 4.1. Without additional DI water, higher viscosity is achieved which helps to form a thick layer.

Wetting of the separator ink was tried to improve with surface treatment on the electrode layer. The sample that had the current collector and electrode screen-printed was 30 min under N_2 plasma, O_2 plasma, and UV-ozone surface treatment. Figure 19 shows that compared with the untreated sample all surface treatments had negative effects and with O_2 plasma the electrode layer did etch away. Because none of the treatments showed improvements the effect of treatment was not investigated further. In the case of the 30 min treatment with oxygen plasma, the electrode layer was lost. Therefore, lower treatment time could save the electrode layer, but might not bring any improvement for the separator print.

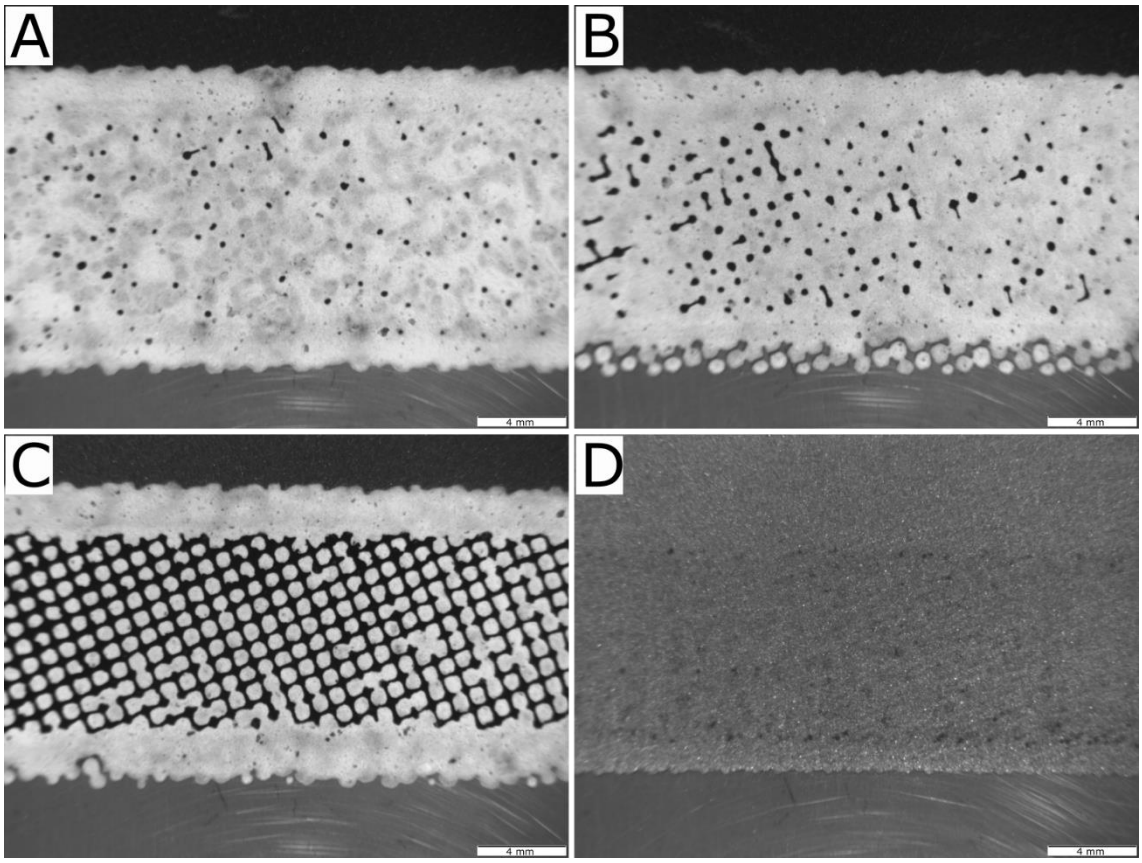

Figure 19. *Surface treatment on the bottom electrode layer. A, untreated. B, UV-ozone. C, N_2 plasma. D, O_2 plasma. Scale bars are 4 mm.*

With the screen NBC EX 12-150 a single print was not enough to form a uniform separator layer, so multiple prints were tested. Separator was formed with a single print followed by curing, and a double print followed by curing. Also, the used screen-printer enables offset for alignment. Therefore, the double print was tested also with an offset value for the second print. After the first curing, the separator layer had holes and therefore printing was repeated on top of the earlier separator layer. Thus, two times repeated separator layer has four prints (2+2) and three times repeated has six prints (2+2+2).

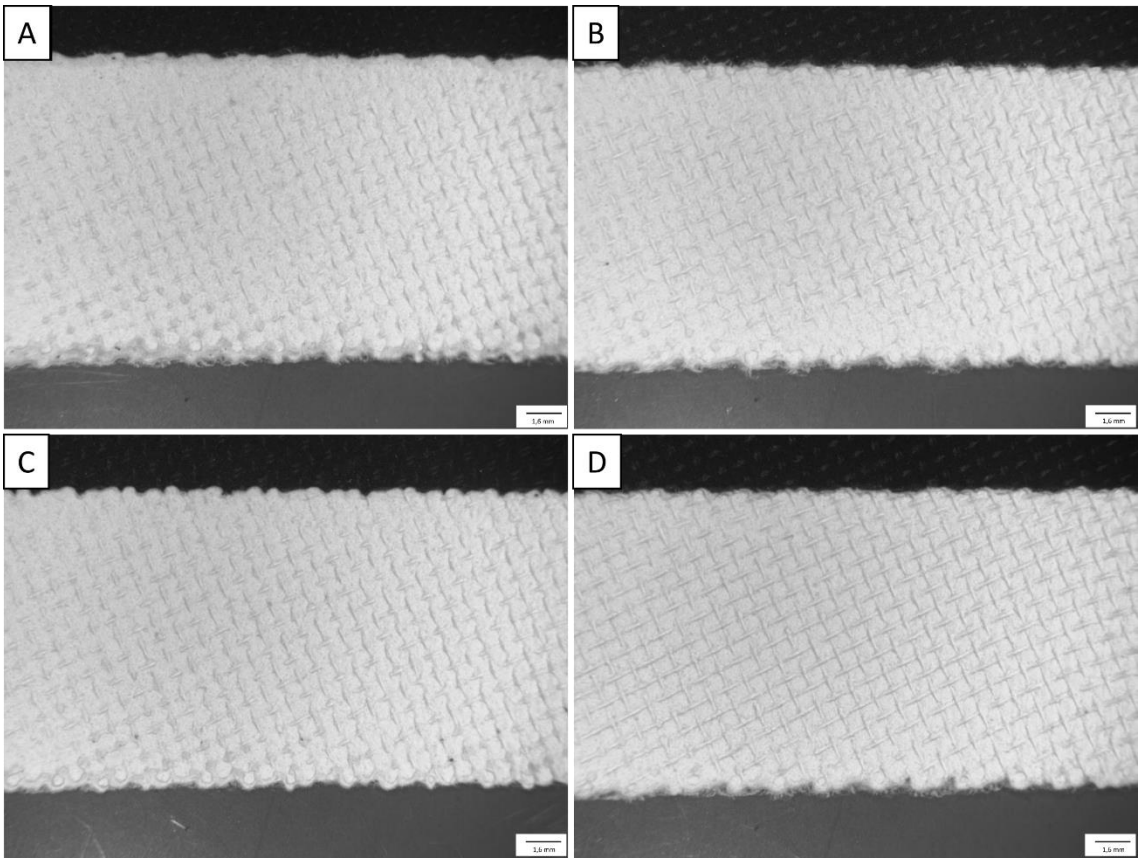

Figure 20. *A, 2+2 print. B, 2+2+2 print. C, 2+2 print with offset. D, 2+2+2 print with offset. Scale bars are 1.6 mm.*

Small changes from the initial printing parameters were tested, but only forward pressure was observed to bring improvement. After multiple prints, the mesh pattern can be seen on the separator layer. However, reduced pressure can minimize the traces on the separator layer and thus, 150 N was used in the Printing pressure forward setting. The best separator layer with the screen NBC EX 12-150 was got when printed twice before curing and then repeated two or three times. The effect of the offset was not tested for screens NBC EX 24-125 and 31-071, because with screen 12-150, similar uniform layers were got with and without the offset as seen in Figure 20. Additionally, the printing process is simpler without the offset as it is not needed to change for every print.

Table 7. Tested prints for the separator layer with different screens.

Prints	**NBC EX 12-150**	**NBC EX 24-125**	**NBC EX 31-071**
1	Faulty	Faulty	Faulty
1+1	Faulty	Faulty	Faulty
1+1+1	Faulty	Faulty	OK
2	Faulty	Faulty	Faulty
2+2	OK	Faulty	OK
2+2+2	OK	OK	OK
(With offset) 2	Faulty	Not tested	Not tested
(With offset) 2+2	OK	Not tested	Not tested
(With offset) 2+2+2	OK	Not tested	Not tested

Three different screens were available for printing the separator layer and were tested with different printing sequences that are presented in Table 7. In the table samples that had holes in the layer are marked as Faulty. OK-mark was given for every sample that was found to have a uniform layer viewed by bare eyes. Samples that looked uniform and could prevent contact between the electrodes were viewed with the stylus profilometer. Measurement data were used to calculate average and RMS roughness with equations 7 and 8. Hence, the roughness of the layers was found and compared with each other in Table 8. When the prints are repeated the roughness will increase, but the printing times before the curing do not have an effect. Roughness comes mostly from the mesh pattern that is left on the layer after the last print. Hence, the screen with a smaller thread diameter gives the smoothest layer. It is expected that printing of the top electrode could be easier and more regular on the smooth separator layer rather than on the rough layer.

Table 8. Roughness of different separator layers.

Screen	**Print**	**R_a (µm)**	**RMS (µm)**
NBC EX 12-150	2+2	17.19	21.93
	2+2+2	21.72	29.85
	(With offset) 2+2	20.16	27.67
	(With offset) 2+2+2	26.10	35.36
NBC EX 24-125	2+2+2	14.19	18.58
NBC EX 31-071	1+1+1	10.64	14.55
	2+2	9.99	12.83
	2+2+2	10.70	14.13

Two screens with different printing sequences were then used to fabricate monolithic supercapacitors. Screen 31-071 was used with a 2+2+2 print sequence and for screen 12-150 print sequence of 2+2 with offset was used. Both combinations produced separator layers with an average thickness of approximately 100 µm. Dry resistance was measured and used to evaluate yield for the supercapacitors and successful separator layer. With the screen 31-071, twelve samples were fabricated, and the lowest measured resistance was 600 kΩ. Therefore, all twelve samples were successful and the separator yield was 100%. With the screen 12-150 in total 36 samples were fabricated, but only 13 had higher dry resistance than 3.5 kΩ. This leads to 36% yield for the supercapacitor that had a separator made with the screen 12-150. As screen 31-071 with printing sequence 2+2+2 provided a high yield for the separator layer it was selected as the process for the demonstrated monolithic supercapacitors. Although the demonstrated separator prevented short circuits, small holes are observed in the layer as illustrated in Figure 21. The diameter of the holes is approximately 10 µm, but it is not clear if any of these holes pass the whole layer.

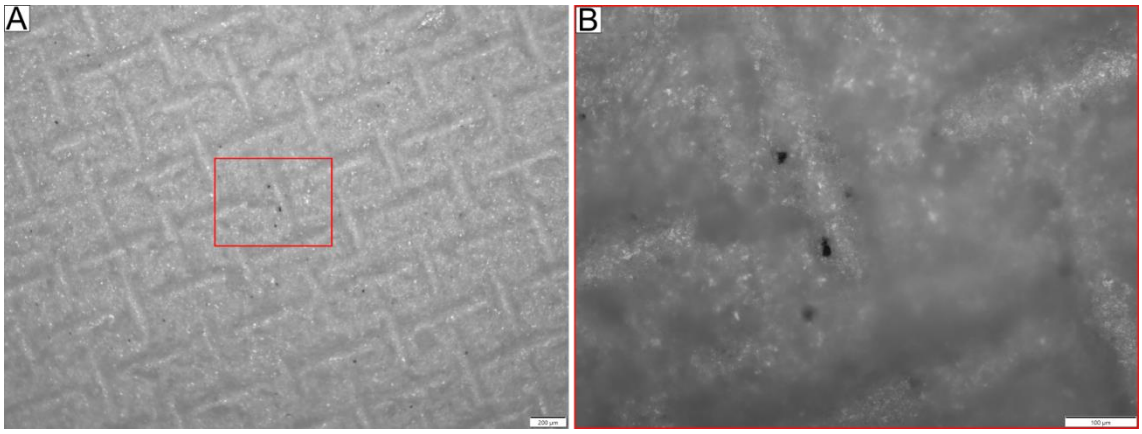

Figure 21. *Separator screen-printed with screen NBC EX 31-071 (2+2+2). The scale bar is 200 µm in figure A and 100 µm in figure B.*

5.2 Results of the fabricated supercapacitors

Supercapacitors were fabricated as single-cells and modules. Blade coating was used only for single-cell supercapacitors. Screen-printing was used to fabricate modules as well as single-cell supercapacitors. Different blade coated supercapacitors were compared with each other, and single-cell supercapacitors with monolithic structures were compared with each other. Furthermore, supercapacitor modules were examined to evaluate the performance and suitability of the screen-printing process of monolithic supercapacitors.

Electrical characterization was done with a voltage of 1.2 V for all individual cells. The modules of three cells were measured with a voltage of 3.3 V. Used currents were the same for all supercapacitors. The capacitance was defined with a discharge current of 1 mA and the ESR was defined with a current of 10 mA. The specific capacitance reported is obtained from device capacitance divided by total electrode mass.

5.2.1 Blade coated single-cell supercapacitors

Two different structures were used in supercapacitors with a single-cell. Monolithic and F2F structures were fabricated by blade coating and compared with each other. For comparison capacitance, ESR, leakage current, and specific capacitance are used. Results of the blade coated supercapacitors with F2F structure are presented in Table 9 and with monolithic structure in Table 10. A comparison of the results of the blade coated single-cell supercapacitors is illustrated in Figure 22. Both structures have six samples which are combined from two different fabrication batches. Generally, the fabrications of the blade coated supercapacitors were successful even though the first three samples with the monolithic structure had high leakage currents. Also, both structures with the blade coating had some samples with cracks on the electrodes.

Table 9. Blade coated supercapacitors with face-to-face structure.

Sample	Capacitance (mF)	ESR (Ω)	Leakage current (µA)	Specific capacitance (F/g)
1	188.8	20.5	5.6	11.7
2	187.1	21.3	5.4	11.7
3	181.0	18.0	5.3	11.0
4	193.6	17.9	5.7	11.9
5	188.8	18.0	5.8	11.8
6	192.3	17.2	5.7	12.2
Mean	188.6	18.8	5.6	11.7
σ	4.4	1.6	0.2	0.4

Table 10. Blade coated supercapacitors with monolithic structure.

Sample	Capacitance (mF)	ESR (Ω)	Leakage current (µA)	Specific capacitance (F/g)
7	181.7	26.5	19.0	10.2
8	174.4	28.3	40.2	9.3
9	171.3	39.0	170.8	9.1
10	181.8	33.4	4.9	10.4
11	184.4	30.4	8.1	10.6
12	178.6	32.0	5.0	9.7
Mean	178.9	31.6	41.3	9.9
σ	4.9	4.4	64.8	0.6

Monolithic samples 7 and 8 had less viscous separator ink which was previously used in the screen-printing and could be a reason for higher leakage current. The leakage current of the monolithic sample 9 is the highest, but the rest of the samples have the expected value. During the blade coating, some agglomerates or bubbles have been observed which could be the cause for the high leakage current. Nevertheless, the coated separator can prevent contact as a thick layer. On the other hand, the F2F supercapacitors have similar leakage currents together. Thus, the use of the paper separator can provide a more repeatable supercapacitor than the blade coated separator.

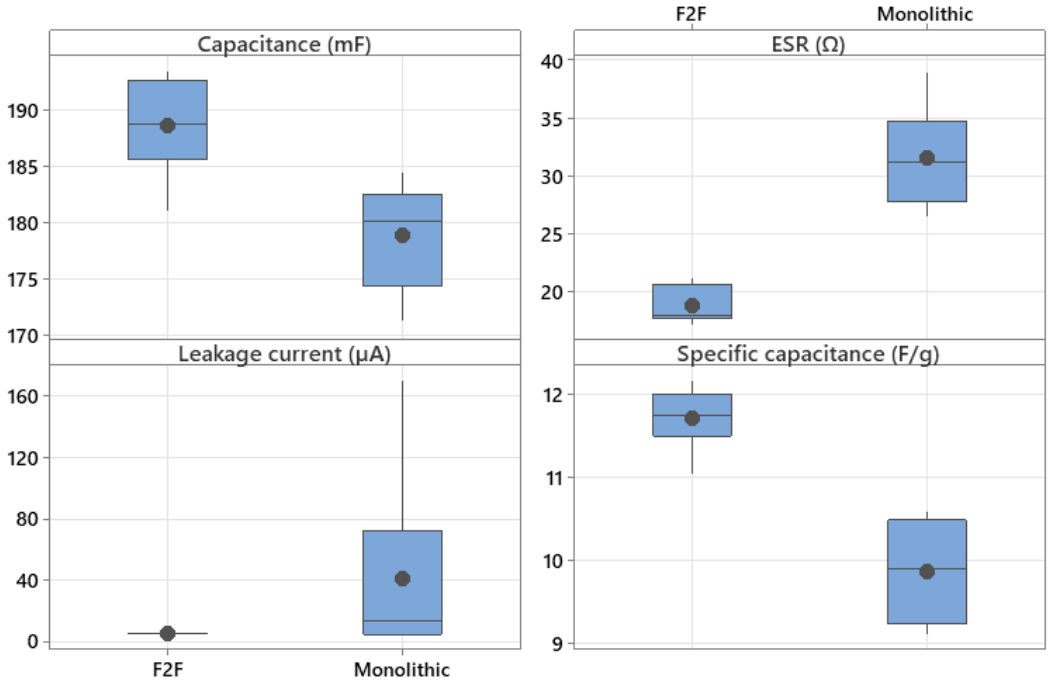

Figure 22. *Boxplot of the blade coated supercapacitors with face-to-face and monolithic structure. The mean value marked with a circle and the median with a horizontal line.*

Structures have clear differences between the ESRs as seen in Figure 22. The F2F structure has two similar current collectors, but the monolithic structure has a slightly narrower top current collector. In addition to that the thickness of the upper current collector on top of the other layers is thinner than the bottom current collector on the monolithic sample as illustrated in Figure 23. The thinner and narrower top current collector could explain why the ESR of the monolithic supercapacitors is higher than the ESR of the F2F supercapacitors. Capacitances of the supercapacitors are slightly smaller with a monolithic structure versus the F2F structure. Even though capacitance is higher with the F2F structure the deviations are similar between the structures, the standard deviation (σ) for F2F is 4.4 and for monolithic 4.9. The deviations of specific capacitance are similar, even though electrodes for the F2F structure were selected so that the total mass of two electrodes would be as close as possible to the others.

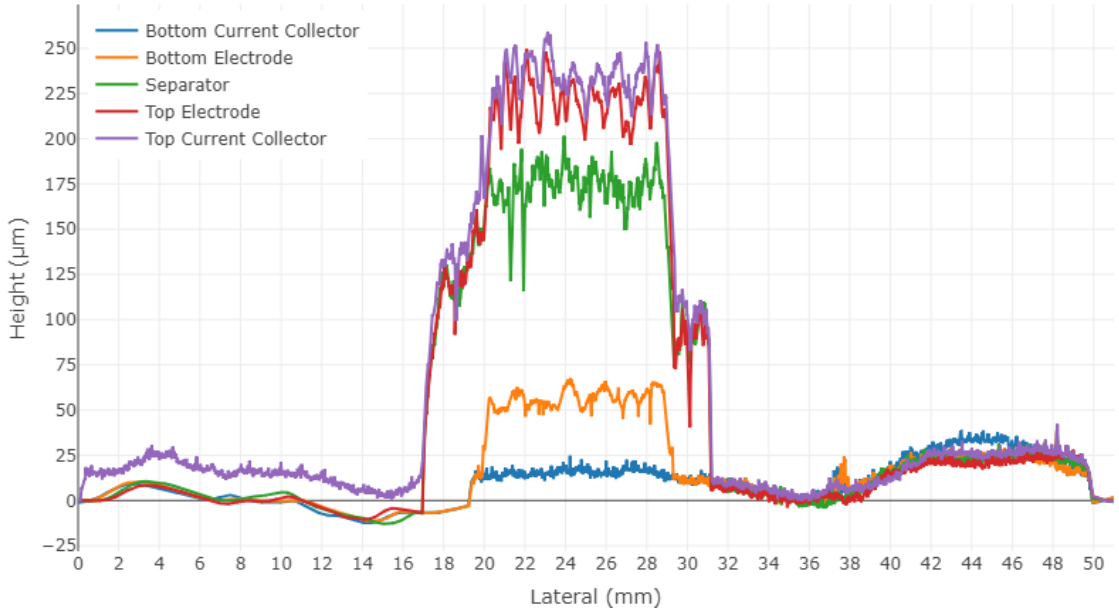

Figure 23. *Cross section of the blade coated monolithic supercapacitor.*

5.2.2 Monolithic single-cell supercapacitors

Screen-printing was used to fabricate twelve monolithic supercapacitors. The separator was made with the screen 31-071 with printing sequence 2+2+2 as it was discovered to be successful. Other layers were made as described in Chapter 4.3. All twelve fabricated samples were characterized and capacitance, ESR, leakage current, and specific capacitance are presented in Table 11. In Figure 24 all monolithic single-cell supercapacitors are presented together, blade coated from Table 10 and screen-printed from Table 11.

Table 11. Screen-printed single-cell supercapacitors with monolithic structure.

Sample	Capacitance (mF)	ESR (Ω)	Leakage current (µA)	Specific capacitance (F/g)
13	135.7	19.9	3.3	9.2
14	116.0	22.5	4.5	8.8
15	151.0	25.3	4.7	9.0
16	139.5	22.7	4.2	9.0
17	146.3	22.8	5.0	9.1
18	141.4	22.9	5.6	8.9
19	146.7	20.1	4.7	9.3
20	142.3	19.7	5.0	9.1
21	157.0	20.0	5.6	9.1
22	152.1	22.3	5.3	9.2
23	139.9	21.6	2.5	9.5
24	127.1	23.1	4.4	9.1
Mean	141.3	21.9	4.6	9.1
σ	11.2	1.7	0.9	0.2

All fabricated samples turned out to be successful and functional supercapacitors. In the printing, the bottom electrode was observed to have a similar mass across the samples.

On the other hand, the top electrode mass had more variation between the samples. Also, during the printing it was observed that some samples had the separator layer visible through small holes in the top electrode layer. With the blade coated samples, the variation of electrode mass is smaller than with the screen-printed samples. Therefore, the higher deviation of capacitance in screen-printed samples can be explained by the top electrode. The total electrode mass is also smaller with the screen-printed samples and so it is understandable that the capacitance is smaller compared with the blade coated samples. Specific capacitance has a smaller variation with the screen-printed samples. As the electrode mass corresponds better to the capacitance, low mass is for low capacitance. On the other hand, the blade coated samples with high mass correspond to low capacitance and vice versa. However, it is unclear if the source for this is poor alignment or some other unidentified factor.

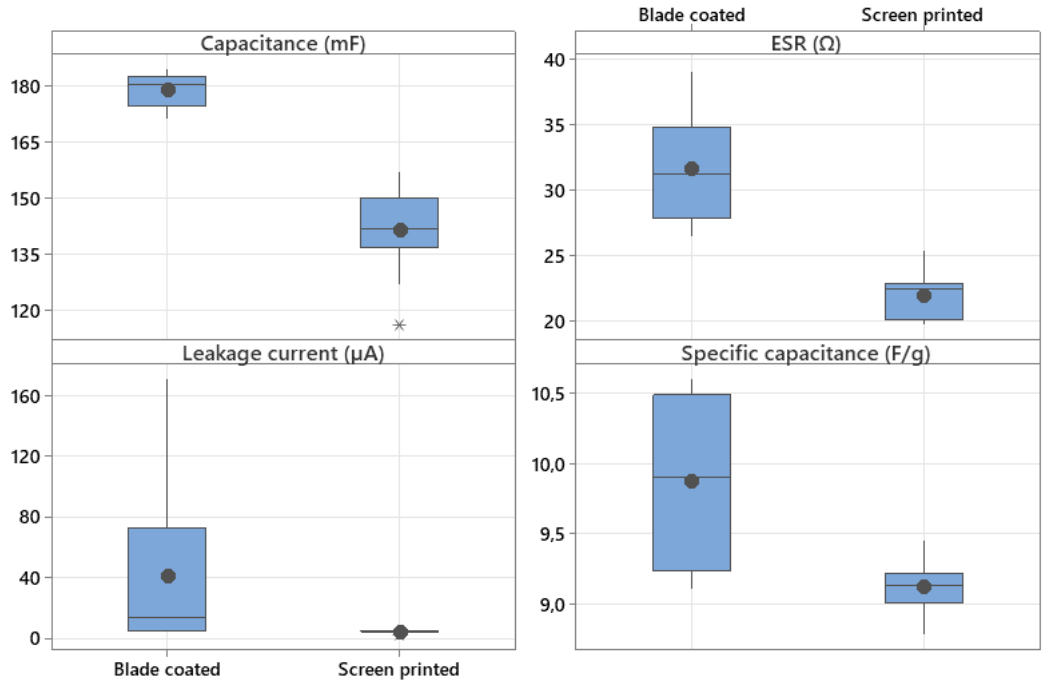

Figure 24. *Blade coated and screen-printed monolithic single-cell supercapacitors. The mean value marked with a circle and the median with a horizontal line.*

Screen-printed samples also have a thin upper current collector on top of the other layers as illustrated in Figure 25. From plotted cross-section data it is hard to estimate the difference between the samples. However, the top current collector is 9 mm wider, and the area is 45% bigger for the screen-printed sample. Therefore, the screen-printed supercapacitor can be expected to have a smaller ESR. Furthermore, the screen-printed monolithic supercapacitor has a similar ESR to blade coated F2F supercapacitors and

so it can be deduced that the printed separator does not greatly decrease the ionic conductivity and thus increase ESR.

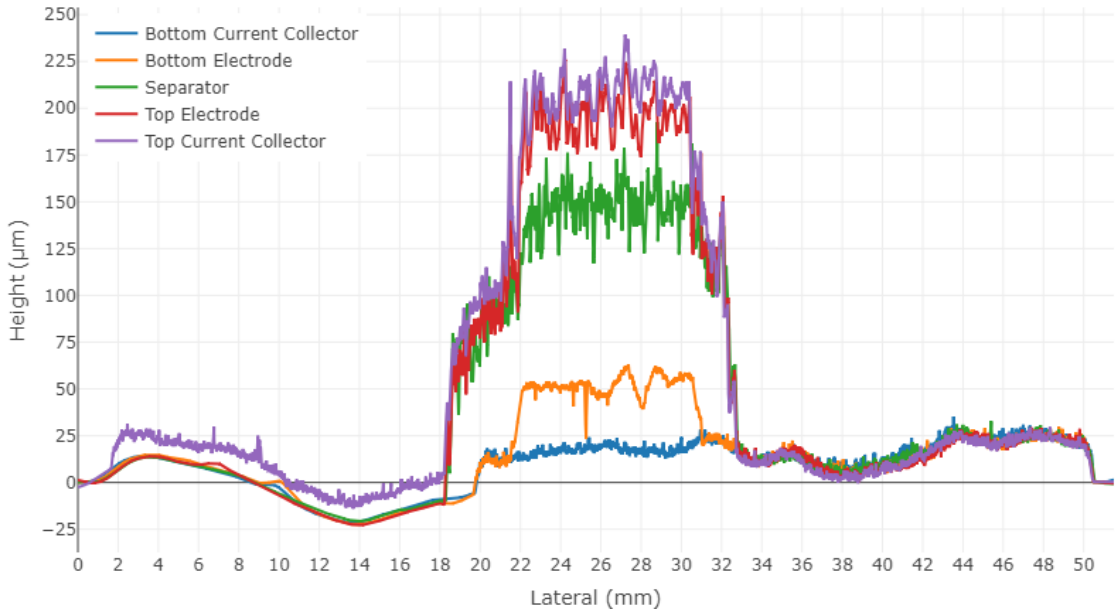

Figure 25. *Cross-section of the screen-printed monolithic supercapacitor.*

The leakage current values of the screen-printed supercapacitors are all small and indicate regular separators between the samples. Blade coated samples have higher variation, but also dry resistance was significantly lower. The lowest measured dry resistance was 3.8 kΩ for blade coated supercapacitors and 600 kΩ for screen-printed supercapacitors. Characterization results and the fact that all fabricated samples turned out to be functional supercapacitors demonstrate the success of the demonstrated printing process.

5.2.3 Screen-printed monolithic three-cell supercapacitor module

Screen-printing of the monolithic single-cell supercapacitors was found to be successful so the same process was used to fabricate supercapacitor modules. Four modules with three supercapacitor cells in the series were fabricated. The characterization of the modules started by characterizing every cell individually with a voltage window of 1.2 V like with the single-cell supercapacitors. The measured capacitance values of the cells in the modules are illustrated in Figure 26. Strangely the first and the last cells in the series have smaller capacitance than the middle one. In the fabrication pipeline, the first two samples have higher capacitance than the last two. Over time the ink dehydrates and starts to cause clogging in the screen. However, the differences between the cells in the module are similar between all samples regardless of the fabrication order. In both

electrode layers, the electrodes of the cells are printed at the same time. While in the single-cell supercapacitors, the top electrode was challenging, in the modules the print was observed to be visually similar and flawless as illustrated in Figure 27. Differences in the mass of electrodes were observed between the samples, but as all electrodes in the layer are printed simultaneously the possible difference between the electrodes stays hidden.

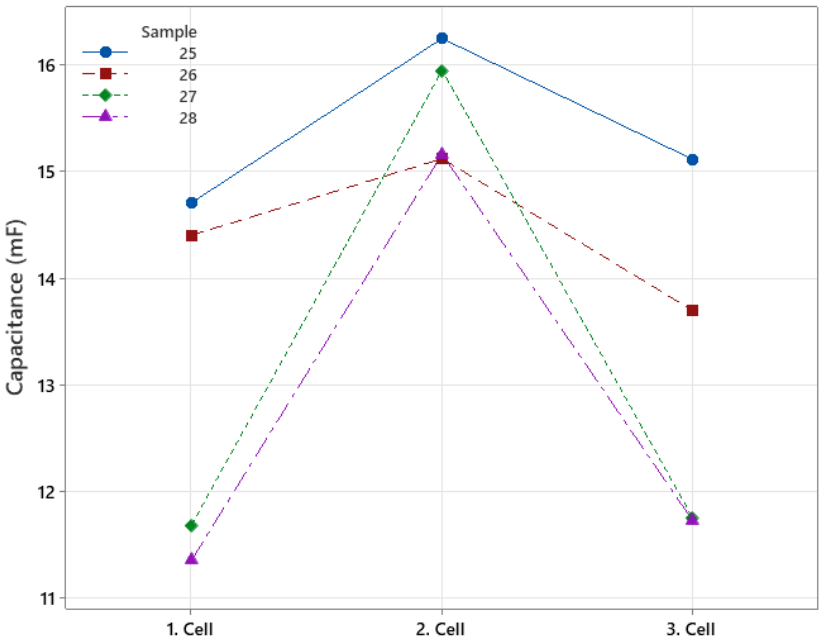

Figure 26. *Capacitance of the cells in the supercapacitor modules.*

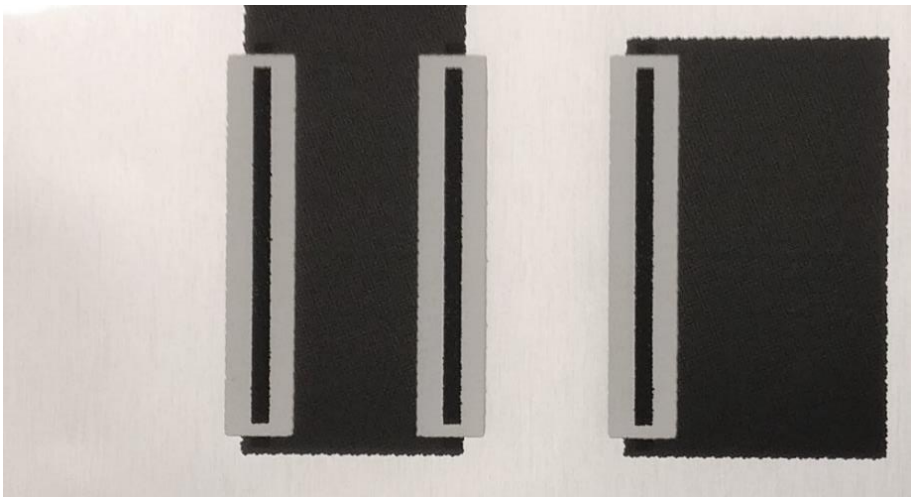

Figure 27. *Top electrodes of the monolithic supercapacitor module.*

Capacitance values differ between the cells in the modules and therefore a lower voltage window than 3.6 V was needed for the modules to avoid excess voltage over the cells with lower capacitance. A voltage of 3.3 V was chosen for the characterization of modules and thus 1.23 V is not exceeded in any cell. For example, in the module 27, all

cells have the same electric charge and the module voltage of 3.3 V. Therefore, the cell with the lowest capacitance (11.7 mF) has a voltage of 1.215 V, and the one with the highest capacitance (15.9 mF) has a voltage of 0.890 V. Characterization results of the modules and capacitances of the cells are presented in Table 12. All four fabricated modules were found to be functional supercapacitors. Low leakage current with all modules demonstrates a successful separator layer as in the single-cell supercapacitors. Printing of the electrodes was successful, but a difference between the samples was observed. The modules have approximately three times higher ESR than the single-cell supercapacitors, as was expected with three cells. Modules had shorter current collectors which decreased ESRs, but at the same time, smaller area of electrodes increased ESRs.

Table 12. Characterization results of the screen-printed supercapacitor modules.

Sample	Capacitance of cell 1 (mF)	Capacitance of cell 2 (mF)	Capacitance of cell 3 (mF)	Total capacitance (mF)	Total ESR (Ω)	Total Leakage current (µA)
25	14.7	16.2	15.1	4.6	56.9	0.63
26	14.4	15.1	13.7	4.4	56.8	0.50
27	11.7	15.9	11.7	3.9	57.3	0.56
28	11.4	15.2	11.7	3.7	61.2	0.38
Mean	13.0	15.6	13.1	4.2	58.1	0.52
σ	1.8	0.6	1.6	0.4	2.1	0.11

The cells were characterized once more three months later, and the results remained mostly the same. The second cell in the module had the highest capacitance compared with other cells. However, sample number 26 had only two working cells, as characterization failed on cell three. Capacitance of the cell three is the smallest in the module, so breakdown could result from too high voltage during the module characterization. Additionally, the failure in the encapsulation could be a reason for the breakdown. Also, poor encapsulation can leave a gap for the electrolyte to dry.

Module with series connections does not work after one cell has failed. To avoid failures, similar capacitances should be aimed between the cells. Additionally, different ESR values have effects on the temperatures of cells and can change the ageing between cells. Slightly higher voltage form rated should not instantly destroy supercapacitors, but it starts gas evolution and encapsulation may break. Failures of cells in modules can be minimized with similar cells and additionally balancing cells passively or actively. The simplest passive balancing is to place bypass resistors in parallel with the cells. [10]

The voltage rating of the series modules without balancing should be based on a cell with the lowest capacitance. Supposed, the maximum voltage (V_{max}) for the cell is 1.2 V and the lowest capacitance is 30% lower than the highest capacitance. Therefore, the highest capacitance cell will have voltage:

$$V = 0.7V_{max}. \quad (9)$$

Equation 4 shows that overall voltage across the module decreases as all cells cannot have maximum voltage. Decreased voltage limits the used voltage but also affects the energy stored in the module. Energy (E) of supercapacitors can be obtained by the following equation:

$$E = \frac{1}{2}CV^2, \quad (10)$$

where C is the total capacitance and V is the voltage across the supercapacitor [10]. In this work, cells were fabricated on the same substrate which prevents choosing individual cells. Thus, by improving the uniformity of the electrode layers a higher voltage across the module could be achieved. Besides electrode ink also the module design should be investigated. The module has currently narrow electrodes. Probably wider electrodes used in the single-cells illustrated in Figure 25 could reduce the difference between cells in the module.

6. CONCLUSIONS AND FUTURE WORK

The main purpose of the work was to fabricate the monolithic supercapacitor using the screen-printing process. Small and regular leakage current with functional supercapacitors from all fabricated samples indicates the success of the screen-printing process. Monolithic supercapacitors have 5 layers and for screen-printed samples, the separator is printed 6 times. In addition to the multiple prints, screen mesh size and ink viscosity were found to be crucial for printed separators. In total, the supercapacitor requires 10 prints and those need to be aligned to the top of the others. The automated alignment in the screen-printer ensures that all layers are aligned correctly, and the effect of the operator stays minimal. With the blade coating, the operator has a higher effect as the alignment of the layers is done manually and the polyimide masks can move more easily during the coating.

In the supercapacitor fabrication, similar printing results were achieved even though air humidity changed. The highest concern was the separator layer in the monolithic structure, but in this work, a reliable separator was fabricated with screen-printing. The average leakage current of the supercapacitors was found to be 4.6 µA with the printed separator and compared to 5.6 µA with the paper separator. Furthermore, the ESR values were similar compared to the F2F supercapacitors. The separator and the electrode inks have the same binder and thus the solvent in the upper layer could dissolve the layer underneath. For example, when the top electrode is printed the solvent of the binder can start to dissolve the separator layer. One desired feature for the separator layer is porosity and the electrode ink could as well leak through those pores. From these results, it is hard to estimate if the pores pass the ink through or if the printed ink dissolves the underneath layers.

The results of this work do not answer for the variations observed between the electrodes and thus in the capacitance of the samples. One potential cause could be the drying rate of the electrode ink. The solvent of the electrode ink has a significant effect on printing, as it prevents the clogging of the screen. Even though the ink did not completely clog the openings of the screen, over time the ink dried at the edges and affected output. Therefore, screen-printing of the monolithic supercapacitor should next attend to improve the printability of the electrode ink, as with optimized ink more regular capacitors could be achieved. With better control for the electrode layers, the capacitances of the devices could be closer to each other.

The introduced separator works well, but now the layer is thick and requires multiple prints for a uniform layer to prevent the short circuit. Reducing printing times needed for the separator layer reduces fabrication costs as fewer printings are done and a simpler process. A thinner separator layer on the other hand could improve the bendability of the supercapacitor and improve printability. Additionally, a thinner structure could help the top current collector that is printed from the substrate level on the top of all other layers. Fabrication in this work was implemented with screen-printing on a sheet. The next approach would be to try an R2R process for monolithic supercapacitor fabrication. Ideally, blank substrate fed to process would have completed supercapacitor at the end of the R2R process. Succeeded R2R fabrication could provide high-volume production and lower cost per fabricated unit. [19]

Some of the materials now used for the supercapacitors are already renewable, but also mined materials like talc and aluminium are used. Both mined materials are common and can be recycled, nevertheless new supply is needed to mine. [26,27] It is important to keep investigating novel materials and combinations to fabricate even more sustainable supercapacitors. Further the materials need optimization for different fabrication techniques and structures.

REFERENCES

[1] M. Şahin, F. Blaabjerg, A. Sangwongwanich, A Comprehensive Review on Supercapacitor Applications and Developments, Energies, 2022, Vol. 15, Iss. 3, 674 p., Available: doi.org/10.3390/en15030674.

[2] V. Molahalli, K. Chaithrashree, M. K. Singh, M. Agrawal, S. G. Krishnan, G. Hegde, Past decade of supercapacitor research – Lessons learned for future innovations, Journal of Energy Storage, 2023, Vol. 70, Iss. 15, Available: doi.org/10.1016/j.est.2023.108062.

[3] A. K. Samantara, S. Ratha, Materials Development for Active/Passive Components of a Supercapacitor, Springer Singapore, 2018, Available: doi.org/10.1007/978-981-10-7263-5.

[4] Y. S. Cho, K. Choi, J. Kwon, Self-sustainable wireless sensor network for low-temperature application, Micro & Optical Tech Letters, 2022, Vol. 64, Iss. 2, pp. 305–11, Available: doi.org/10.1016/j.est.2018.02.008.

[5] N. I. Jalal, R. I. Ibrahim, M. K. Oudah, A review on Supercapacitors: types and components, J Phys: Conf Ser, 2021, Vol. 1973, Available: doi.org/10.1088/1742-6596/1973/1/012015.

[6] J. Zhang, G. Zhang, T. Zhou, S. Sun, Recent Developments of Planar Micro-Supercapacitors: Fabrication, Properties, and Applications, Adv. Funct. Mater., 2020, Vol. 30, Iss. 19, Available: doi.org/10.1002/adfm.201910000

[7] J. Keskinen, A. Railanmaa, D. Lupo, Monolithically prepared aqueous supercapacitors, Journal of Energy Storage, 2018, Vol. 16, pp. 243–249, Available: doi.org/10.1016/j.est.2018.02.008

[8] M. A. Scibioh, B. Viswanathan, Materials for supercapacitor applications, Elsevier, 2020.

[9] B. E. Conway, Electrochemical Supercapacitors: Scientific Fundamentals and Technological Applications, Springer, 1999.

[10] A. Yu, V. Chabot, J. Zhang, Electrochemical Supercapacitors for Energy Storage and Delivery: Fundamentals and Applications, CRC Press, 2017, Available: doi.org/10.1201/b14671

[11] S. Zhang, N. Pan, Supercapacitors Performance Evaluation, Adv. Energy Mater., 2015, Vol. 5, Iss. 6, Available: doi.org/10.1002/aenm.201401401.

[12] C. Zhong, Y. Deng, W. Hu, D. Sun, X. Han, J. Qiao, J. Zhang, Electrolytes for Electrochemical Supercapacitors, CRC Press, 2016, Available: doi.org/10.1201/b21497.

[13] W. Raza, F. Ali, N. Raza, Y. Luo, K.-H. Kim, J. Yang, S. Kumar, A. Mehmood, E. E. Kwon, Recent advancements in supercapacitor technology, Nano Energy, 2018, Vol. 52, pp. 441–473, Available: doi.org/10.1016/j.nanoen.2018.08.013

[14] K. K. Kar (editor), Handbook of Nanocomposite Supercapacitor Materials I: Characteristics, Springer Cham, 2020, Available: doi.org/10.1007/978-3-030-43009-2.

[15] C. Zhong, Y. Deng, W. Hu, J. Qiao, L. Zhang, J. Zhang, A review of electrolyte materials and compositions for electrochemical supercapacitors, Chem Soc Rev, 2015, Vol. 44, Iss. 21, pp. 7431–7920, Available: doi.org/10.1039/C5CS00303B

[16] J. Li, H. Jia, S. Ma, L. Xie, X.-X. Wei, L. Dai, H. Wang, F. Su, C.-M. Chen, Separator Design for High-Performance Supercapacitors: Requirements, Challenges, Strategies, and Prospects, ACS Energy Lett, 2023, Vol. 8, Iss. 1, pp. 56–78, Available: doi.org/10.1021/acsenergylett.2c01853.

[17] J. Wiklund, A. Karakoç, T. Palko, H. Yiğitler, K. Ruttik, R. Jäntti, J. Paltakari, A Review on Printed Electronics: Fabrication Methods, Inks, Substrates, Applications and Environmental Impacts, Journal of Manufacturing and Materials Processing, 2021, Vol. 5, Iss. 3, 89 p., Available: doi.org/10.3390/jmmp5030089.

[18] C. H. Rao, K. Avinash, B. K. S. V. L. Varaprasad, S. Goel, A Review on Printed Electronics with Digital 3D Printing: Fabrication Techniques, Materials, Challenges and Future Opportunities, Journal of Electronic Materials, 2022, Vol. 51, pp. 2747–2765, Available: doi.org/10.1007/s11664-022-09579-7.

[19] Y.-Z. Zhang, Y. Wang, T. Cheng, L.-Q. Yao, X. Li, W.-Y. Lai, W. Huang, Printed supercapacitors: materials, printing and applications, Chem Soc Rev, 2019, Vol. 48, Iss. 12, pp. 3229–3264, Available: doi.org/10.1039/C7CS00819H.

[20] F. C. Krebs, Fabrication and processing of polymer solar cells: A review of printing and coating techniques, Solar Energy Materials and Solar Cells, 2009, Vol. 93, Iss. 4, pp. 394–412, Available: doi.org/10.1016/j.solmat.2008.10.004.

[21] X. Peng, L. Peng, C. Wu, Y. Xie, Two dimensional nanomaterials for flexible supercapacitors, Chem. Soc. Rev., 2014, Vol. 43, Iss. 10, pp. 3303-3323, Available: doi.org/10.1039/C3CS60407A.

[22] X. Shi, S. Pei, F. Zhou, W. Ren, H.-M. Cheng, Z.-S. Wu, X. Bao, Ultrahigh-voltage integrated micro-supercapacitors with designable shapes and superior flexibility, Energy Environ. Sci., 2019, Vol. 12, Iss. 5, pp. 1534–1541, Available: doi.org/10.1039/C8EE02924E.

[23] S.-J. Potts, C. Phillips, E. Jewell, B. Clifford, Y. C. Lau, T. Claypole, High-speed imaging the effect of snap-off distance and squeegee speed on the ink transfer mechanism of screen-printed carbon pastes, J Coat Technol Res, 2020, Vol. 17, Iss. 2, pp. 447–59, Available: doi.org/10.1007/s11998-019-00291-6.

[24] B. Bhushan, Introduction to Tribology, John Wiley & Sons Incorporated, 2013, 14–22 p.

[25] UV Ozone Cleaning for AFM SEM TEM, Wafers, Glass, PDMS & more, Novascan, website, (accessed on Aug 7 2023), Available: https://www.novascan.com/products/uv_ozone_cleaners_silicon_glass_wafers.php

[26] European Commission, Directorate-General for Internal Market, Industry, Entrepreneurship and SMEs, G. Blengini, C. El Latunussa, U. Eynard, et al., Study on the EU's list of Critical Raw Materials (2020) : critical raw materials factsheets, Publications Office, 2020, Available: doi.org/10.2873/92480.

[27] European Commission, Directorate-General for Internal Market, Industry, Entrepreneurship and SMEs, B. Silvia, G. Blengini, C. El Latunussa, U. Eynard, et al., Study on the

EU’s list of Critical Raw Materials (2020) : factsheets on non-critical raw materials, Publications Office, 2020, Available: doi.org/10.2873/587825.